arXiv:1403.6974v1 [cs.IT] 27 Mar 2014

DIPP - Distributed Parallel Pursuit

Dennis Sundman*, *Student Member, IEEE,* Saikat Chatterjee, *Member, IEEE,*
and Mikael Skoglund, *Senior Member, IEEE*

***Abstract*—We consider a distributed compressed sensing scenario where multiple sensors observe correlated sparse signals and the sensors are connected through a network. The signal correlation is realized by a partial common support-set. For such a system, the main objective of this paper is to develop a greedy pursuit algorithm. To fulfill the objective, we develop distributed parallel pursuit algorithm and provide restricted isometry property based analysis on convergence and reconstruction performance. Through simulations we show that the distributed parallel pursuit provides a good performance for a reasonably connected network.**

***Index Terms*—Compressed sensing, distributed processing.**

I. Introduction

Compressed sensing (CS) [2], [3] refers to a class of undersampling problems, where the sampled (or measured) data is inherently sparse. A standard CS problem typically considers a single-sensor scenario, where the main task is reconstruction of a large-dimensional signal-vector from a small-dimensional measurement-vector by using a-priori knowledge that the signal is sparse in a known domain. Several CS reconstruction algorithms have been developed in the literature, for example convex optimization- [4], [5] and Bayesian- [6], [7] algorithms. An important class of reconstruction algorithms is the greedy pursuits (GP). From a measurement vector, the GP algorithms use linear algebraic tools to estimate the underlying support-set of the sparse signal-vector followed by estimating associated signal values; here we mention that good support-set estimation is a fundamental aspect for the GP algorithms. Considering support-set estimation strategy, GP algorithms can be categorized in two broad classes: sequential and parallel. A sequential strategy estimates a support-set by finding elements of the support-set one-by-one over iterations. On the other hand, parallel strategy estimates all elements of a support-set simultaneously in an iteration, but improves the support-set estimate over iterations. For example, the sequential types include matching pursuit [8], orthogonal matching pursuit (OMP) [9], and their variations [10], [11], [12], [13]. On the other hand, parallel types include CoSaMP [14], subspace pursuit (SP) [15] and their variations [16]. The GP algorithms are popular due to their low complexity as well as good performance. For any CS reconstructor, providing theoretical reconstruction guarantees with corresponding system requirements are desired features.

In this paper, we consider a distributed (or de-centralized) CS (DCS) problem where multiple sensors are connected over a network. In such a networked scenario, the DCS problem is concerned with reconstructing correlated sparse signals from the random measurements collected in each sensor node. The DCS problem can be solved either in a central manner (by a fusion center) or distributively, the latter which we refer as a DCS solver. There are many results considering centralized CS solvers, for example [17], [18], [19], [20], [21], [22]; and in the class of convex algorithms there are some results for DCS solvers, for example [4], [23], [24], [25]. DCS has a wide range of application areas, for example, distributed sensor perception [26] and distributed spectrum estimation [24], [23], [25], [27]. We refer to a setup as a DCS setup where a DCS problem is solved using a DCS reconstruction algorithm. For such DCS setups, we note that a limited endeavor has been made in literature to develop DCS algorithms based on GP principles. In this regard, our earlier attempts are in [28], [29], [30] and some attempts by others are in [31], [32]. The limited endeavor may be attributed to the lack of theoretical results.

Noting the important role of support-set estimation in GP algorithms, we use the recent mixed support set signal model of [29], [30] that considers correlation over support-sets of all underlying sparse signals in a DCS problem. The correlation is modeled by existence of a partial common (or joint) support-set; the common support-set is a subset of all individual supports of all sparse signals. Using the mixed support set model and appropriate assumptions about system setup, our contributions in this paper are:

- Development of a distributed GP algorithm.
- Analytical study of performance in the sense of provable reconstruction guarantees.

The new algorithm is referred to as *distributed parallel pursuit* (DIPP) and it consists of two main parts: local CS reconstruction, and data fusion. The task of the fusion is, by using the principle strategy of democratic voting, to provide an estimation of the correlation (i.e., estimation of the common support-set), while the local CS reconstruction algorithm use the output from the fusion as side information to improve reconstruction performance. We choose the parallel pursuit algorithm SP and extend it to an algorithm that can use the side information from the fusion algorithm. This algorithm is called SIPP (parallel pursuit with side information) and it is used as the local CS reconstructor. DIPP works iteratively, where it improves the estimation of correlation by exchanging relevant information over the network. While we develop SIPP by extending SP, we could have used other parallel pursuit algorithms such as CoSaMP instead of SP to form SIPP. Using restricted isometry property (RIP) based analysis, we show that under certain theoretical requirements on the sensors and connecting networks, the DIPP algorithm converges to a result

The authors are with the Communication Theory Department, KTH Royal Institute of Technology, 10044 Stockholm, Sweden e-mail: (denniss@kth.se, sach@kth.se, and skoglund@kth.se).

This paper was presented in part at 1st IEEE Global Conference on Signal and Information Processing 2013 [1].

that only depends on a noise term (convergence in theory). We are aware that the RIP based requirements are worst case in nature. In practice, the algorithm iterates until the correlation estimation saturates (convergence in practice) - this happens when further information exchange does not help. We show the practical performance for DIPP by simulations.

The remaining parts of the paper are organized as follows. In section II, we formally define the DCS problem, the signal model and network model. Section III deals with developing DIPP. In section IV, we derive performance bounds and reconstruction guarantees for DIPP. Lastly, in section V, we perform practical evaluation of the DIPP algorithm.

A. Notations and Preliminaries

For enumerating sensor-nodes in the DCS setup, we will reserve sub-indices 'p', 'q' and 'r'. However, to keep the paper clean from notational clutter, we will only use these sub-indices when it is necessary for the discussion. We reserve sub-indices 'l' and 'k' for denoting iteration counter in inner- and outer loops, respectively. Typically, 'l' associates with the iteration counter of SIPP and 'k' associates with DIPP.

Calligraphic letters are used for sets; in particular $\mathcal{T}$, $\mathcal{J}$ and $\mathcal{I}$ denote support-sets while $\mathcal{L}$ is a set of sensor nodes. We denote the full support set, $\Omega \triangleq \{1, 2, \ldots, N\}$. Using Ω, we define the complement $\mathcal{T}^{\mathsf{c}} \triangleq \Omega \setminus \mathcal{T}$. If an algorithm at node p estimates the support-set, this estimate is denoted by $\hat{\mathcal{T}}_{\mathsf{p}}$. $\mathbf{x}_{\mathcal{T}}$ may refer to two things; either $\mathbf{x}_{\mathcal{T}}$ may be the non-zero sub-vector of $\mathbf{x}$ (i.e., $\mathbf{x}_{\mathcal{T}} = \{x_i : i \in \mathcal{T}\}$), or $\mathbf{x}_{\mathcal{T}}$ may be a zero-padded signal, where $\mathbf{x} \in \mathbb{R}^N$, $\mathbf{x}_{\mathcal{T}} \neq 0$ and $\mathbf{x}_{\mathcal{T}^{\mathsf{c}}} = 0$. Which one of these referred to will be clear from the context. When nothing else is stated the norm used is by default the induced ℓ_2-norm (i.e., spectral norm) $\|\cdot\| \triangleq \|\cdot\|_2$. We define the pseudo-inverse for a matrix $\mathbf{A}$ as $\mathbf{A}^{\dagger} \triangleq (\mathbf{A}^*\mathbf{A})^{-1}\mathbf{A}^*$ (where full column rank is assumed) .

We now introduce some existing definitions and results for the standard CS setup, that we will later use for the DCS setup. In standard single-sensor CS:

$$\mathbf{y} = \mathbf{A}\mathbf{x} + \mathbf{e}, \tag{1}$$

where $\mathbf{x} \in \mathbb{R}^N$ is a sparse signal, $\mathbf{y} \in \mathbb{R}^M$ is measurement vector, $\mathbf{A} \in \mathbb{R}^{M \times N}$ is measurement matrix and $\mathbf{e} \in \mathbb{R}^M$ is measurement error, and $M < N$.

Definition 1 (RIP: Restricted Isometry Property [33]): A matrix $\mathbf{A}$ satisfies the RIP with Restricted Isometry Constant (RIC) δ_T if

$$(1 - \delta_T)\|\mathbf{x}\|^2 \leq \|\mathbf{A}\mathbf{x}\|^2 \leq (1 + \delta_T)\|\mathbf{x}\|^2 \tag{2}$$

holds for all T-sparse vectors $\mathbf{x}$ where $0 \leq \delta_T < 1$.

Proposition 1 (Proposition 3.1 in [14]): Suppose $\mathbf{A}$ has RIC δ_T. Let $\mathcal{T}$ be a set of T indices or fewer. Then

$$\|\mathbf{A}_{\mathcal{T}}^*\mathbf{y}\| \leq \sqrt{1 + \delta_T}\,\|\mathbf{y}\|\,, \tag{3a}$$

$$\left\|\mathbf{A}_{\mathcal{T}}^{\dagger}\mathbf{y}\right\| \leq \frac{1}{\sqrt{1 - \delta_T}}\,\|\mathbf{y}\|\,, \tag{3b}$$

$$(1 - \delta_T)\,\|\mathbf{x}\| \leq \|\mathbf{A}_{\mathcal{T}}^*\mathbf{A}_{\mathcal{T}}\mathbf{x}\| \leq (1 + \delta_T)\,\|\mathbf{x}\|\,, \tag{3c}$$

$$\frac{1}{1 + \delta_T}\,\|\mathbf{x}\| \leq \left\|(\mathbf{A}_{\mathcal{T}}^*\mathbf{A}_{\mathcal{T}})^{-1}\mathbf{x}\right\| \leq \frac{1}{1 - \delta_T}\,\|\mathbf{x}\|\,. \tag{3d}$$

Proposition 2 (Approximate Orthogonality): Proposition 3.2 in [14] . Suppose $\mathbf{A}$ has RIC δ_T. Let $\mathcal{S}$ and $\mathcal{T}$ be disjoint sets of indices whose combined cardinality does not exceed $S + T$. Then

$$\|\mathbf{A}_{\mathcal{S}}^*\mathbf{A}_{\mathcal{T}}\| \leq \delta_{S+T}. \tag{4}$$

Corollary 1 (Corollary 3.3 in [14]): Suppose $\mathbf{A}$ has RIC δ_T. Let $\mathcal{T}$ be a set of indices, and let $\mathbf{x}$ be a vector. Provided that $T \geq |\mathcal{T} \cup \mathsf{supp}(\mathbf{x})|$,

$$\|\mathbf{A}_{\mathcal{T}}^*\mathbf{A}\mathbf{x}_{\mathcal{T}^{\mathsf{c}}}\| = \|\mathbf{A}_{\mathcal{T}}^*\mathbf{A}_{\mathcal{T}^{\mathsf{c}}}\mathbf{x}_{\mathcal{T}^{\mathsf{c}}}\| \leq \delta_T\|\mathbf{x}_{\mathcal{T}^{\mathsf{c}}}\|. \tag{5}$$

Lemma 1: For the setup (1), if $\hat{\mathcal{T}}$ is the estimate of the support-set of a signal $\mathbf{x}$ and $\hat{\mathbf{x}}$ is constructed by $\hat{\mathbf{x}}_{\hat{\mathcal{T}}} \leftarrow \mathbf{A}_{\hat{\mathcal{T}}}^{\dagger}\mathbf{y}$, $\hat{\mathbf{x}}_{\hat{\mathcal{T}}^{\mathsf{c}}} \leftarrow \mathbf{0}$, then the following relation holds:

$$\|\mathbf{x} - \hat{\mathbf{x}}\| \leq \frac{1}{1 - \delta_{3T}}\|\mathbf{x}_{\hat{\mathcal{T}}^{\mathsf{c}}}\| + \frac{1}{\sqrt{1 - \delta_{3T}}}\|\mathbf{e}\|. \tag{6}$$

We also have that

$$\|\mathbf{x}_{\hat{\mathcal{T}}^{\mathsf{c}}}\| \leq \|\mathbf{x} - \hat{\mathbf{x}}\|. \tag{7}$$

Proof: See appendix A. ∎

1) Some Algorithmic Notations: For clarity in the algorithmic notations, we define three algorithmic functions as follows:

$$\mathsf{supp}(\mathbf{x}, k) \triangleq \{\textit{the set of indices corresponding to the } k \textit{ largest amplitude components of } \mathbf{x}\},$$

and

$$\mathsf{vote}_1(\mathbf{s}, \mathcal{T}) \triangleq \{\forall j \in \mathcal{T},\ \textit{perform } s_j = s_j + 1\},$$

where $\mathbf{s} = [s_1\ s_2\ \ldots s_N]$ and $s_j \geq 0$. Lastly we define

$$\mathsf{res}(\mathbf{y}, \mathbf{A}) \triangleq \mathbf{y} - \mathbf{A}\mathbf{A}^{\dagger}\mathbf{y}, \tag{8}$$

for full column-rank matrices $\mathbf{A}$.

II. Distributed Compressed Sensing Setup

The DCS problem consists of several sensor nodes connected through a network, where the underlying data collected at the nodes are correlated. In this section we first describe the DCS problem, then the correlation model and lastly we introduce the network model.

A. Distributed Compressed Sensing

In DCS, the p'th sensor measures a signal $\mathbf{x}_{\mathsf{p}} \in \mathbb{R}^N$ according to the following relation

$$\mathbf{y}_{\mathsf{p}} = \mathbf{A}_{\mathsf{p}}\mathbf{x}_{\mathsf{p}} + \mathbf{e}_{\mathsf{p}}, \qquad \forall \mathsf{p} \in \mathcal{L}, \tag{9}$$

where $\mathbf{y}_{\mathsf{p}} \in \mathbb{R}^M$ is the measurement vector, $\mathbf{A}_{\mathsf{p}} \in \mathbb{R}^{M \times N}$ is the measurement matrix, $\mathbf{e}_{\mathsf{p}} \in \mathbb{R}^M$ is the measurement noise and $\mathcal{L}$ is a global set containing all nodes in the network. Throughout this paper we use measurement matrices that have unit ℓ_2-norm columns. This setup describes an under-determined system, where $M < N$. $\mathbf{A}_{\mathsf{p}}$ and $\mathbf{e}_{\mathsf{p}}$ are independent both locally and across the network. The signal vector $\mathbf{x}_{\mathsf{p}} = [x_{\mathsf{p}}(1)\ x_{\mathsf{p}}(2)\ \ldots\ x_{\mathsf{p}}(N)]$ is T-sparse, meaning it has T elements that are non-zero. The element-indices corresponding to non-zero values are collected in the support-set $\mathcal{T}_{\mathsf{p}}$, that means $\mathcal{T}_{\mathsf{p}} = \{i : x_{\mathsf{p}}(i) \neq 0\}$ and $|\mathcal{T}_{\mathsf{p}}| = T$. Next we discuss a relevant signal model that introduces correlation between $\{\mathbf{x}_{\mathsf{p}}\}$.

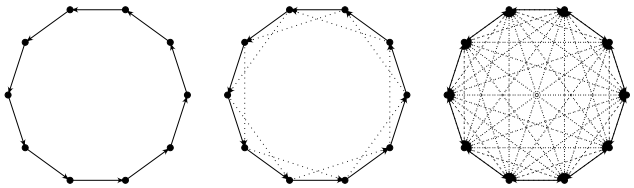

(a) $\mathbf{C}_1$ (b) $\mathbf{C}_2$ (c) $\mathbf{C}_9$

Fig. 1. Three different network topologies.

B. Correlation in Signals: Mixed Support-set Model

We introduce a mixed support-set signal model that brings correlation in signals through their support-sets. This model was previously presented in [22] and [29]. For the sparse signal $\mathbf{x}_\mathsf{p}$, the support-set $\mathcal{T}_\mathsf{p}$ follows the construction

$$\mathcal{T}_\mathsf{p} = \mathcal{I}_\mathsf{p} \cup \mathcal{J}_\mathsf{p} = \mathcal{I}_\mathsf{p} \cup \mathcal{J}, \qquad \forall \mathsf{p} \in \mathcal{L}. \tag{10}$$

Here, the partial support-set $\mathcal{J}_\mathsf{p} = \mathcal{J}$ is joint (i.e., common) to the support-sets of all sparse signals, leading to correlation among signals. The other partial support-set $\mathcal{I}_\mathsf{p}$ is individual and does not incorporate any correlation.

Assumption 1: Denoting $|\mathcal{I}_\mathsf{p}| = I$ and $|\mathcal{J}| = J$, the following assumptions are used throughout the paper:

1) Elements of support-sets are uniformly distributed.
2) $\mathcal{I}_\mathsf{p} \cap \mathcal{J} = \emptyset, \quad \forall \mathsf{p} \in \mathcal{L}$.
3) $\mathcal{I}_\mathsf{p} \cap \mathcal{I}_\mathsf{q} = \emptyset, \quad \forall \mathsf{p}, \mathsf{q} \in \mathcal{L}, \mathsf{p} \neq \mathsf{q}$.
4) Hence, $T = I + J$. □

Additionally, we mention that no correlation between non-zero signal values over $\mathbf{x}_\mathsf{p}$ is assumed. The DIPP estimates $\mathcal{J}$ by cooperation (fusion) through relevant information exchange over a network and gradually improve CS reconstruction performance at each sensor.

We provide few examples of potential real life applications for the mixed support-set model: (1) spectrum estimation - where each node experiences large overlapping supports in the spectrum [27], (2) multiple sensor image capturing - where each node observes the same object from slightly different angles [34], and (3) multiple sensor sound capturing [35]. Also for all the above scenarios and including the one-sensor scenario, if a slowly varying signal is tracked over time, the proposed mixed support-set model may also apply.

C. Network Topology

In DCS, a sensor node is typically unaware of the full network topology. Instead, any node knows two sets of local neighbors; the incoming neighbor connections $\mathcal{L}_\mathsf{p}^{\text{in}}$ and outgoing neighbor connections $\mathcal{L}_\mathsf{p}^{\text{out}}$. Here *incoming* and *outgoing* connections corresponds to communication links where a node can receive or send information, respectively. Using the two sets, consider a number of nodes topologically arranged in a circle. By letting each node forwardly connect to one other node (i.e., node p get $\mathcal{L}_\mathsf{p}^{\text{in}} = \{\mathsf{p}-1\}$ and $\mathcal{L}_\mathsf{p}^{\text{out}} = \{\mathsf{p}+1\}$), a circular topology can be created; we refer to such network as a degree-one network topology. Using ten nodes, we denote the degree-one network by a connection-matrix $\mathbf{C}_1$, depicted in Fig. 1a. A degree-two $\mathbf{C}_2$ network is shown in Fig. 1b and a degree-nine $\mathbf{C}_9$ network is shown in Fig. 1c. We use this structured network topology so that improvement in CS reconstruction performance of DIPP vis-a-vis increase in network connection can be studied in a controlled manner. In this paper we only consider this structured network, although simulation results have shown consistency also for random network models.

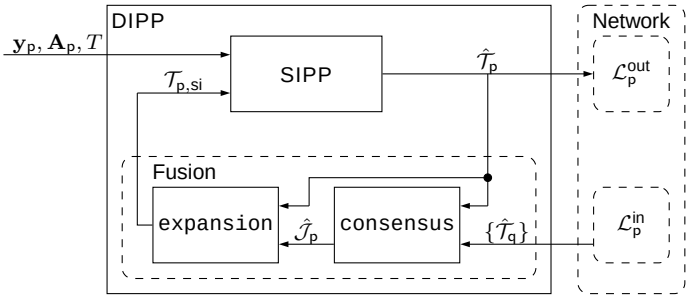

Fig. 2. In this figure, show DIPP and the network. Then, in DIPP, we see the fusion; `consensus` and `expansion` and the local reconstruction algorithm; SIPP.

III. Distributed Parallel Pursuit: Algorithm

Considering the importance of accurate support-set estimation in GP algorithms, we envisage to develop a distributed GP by considering exchange (or communication) of support-set information over the network. By fusing the support-set information and providing the result as side information to SIPP we develop the distributed parallel pursuit (DIPP) algorithm.

A block diagram of DIPP is shown in Fig. 2. DIPP is executed in each node and it comprises of two main parts: (1) a CS reconstruction algorithm - SIPP, and (2) support-set fusion. The fusion comprises of two sub-algorithms: (a) a consensus strategy by voting, and (b) an expansion algorithm. All parts in DIPP are developed to bring the right balance between practical engineering and theory. We describe these parts one-by-one in the following subsections.

A. SIPP: Parallel Pursuit with Side Information

Existing SP algorithm is appropriately modified to develop SIPP, described in algorithm 1. Compared to SP, the modifications are: the supply of $\mathcal{T}_{\mathsf{p},\text{si}}$ as side information satisfying $|\mathcal{T}_{\mathsf{p},\text{si}}| = T$, and the addition of steps 6 to 10 in the iterations of the algorithm. Note the step 7 where $\mathcal{T}_\text{si} = \mathcal{T}_{\mathsf{p},\text{si}}$ participates in CS reconstruction of SIPP. As *stopping criterion*, we can use an upper limit of allowable iterations and/or violation of a non-decreasing residual norm condition, that is if $\|\mathbf{r}_l\| \leq \|\mathbf{r}_{l-1}\|$ violates. Finally, note that if $\mathcal{T}_{\mathsf{p},\text{si}} = \emptyset$ then $\tilde{\mathbf{x}}_l = \hat{\mathbf{x}}_l$, and the SIPP becomes identical to SP.

In DIPP, after execution of SIPP, the support-set estimate $\hat{\mathcal{T}}_\mathsf{p}$ is broadcasted over the network and later fused to estimate common support-set.

B. Fusion

Our fusion strategy has two algorithms: `consensus` and `expansion`. The p'th node has access to support-set estimates $\{\hat{\mathcal{T}}_\mathsf{q}\}_{\mathsf{q} \in \mathcal{L}_\mathsf{p}^{\text{in}}}$ and the local estimate $\hat{\mathcal{T}}_\mathsf{p}$ (provided by the

Algorithm 1 SIPP (parallel pursuit with side information): *Executed in the local node* p

Input: $\mathbf{y}_\mathsf{p}$, $\mathbf{A}_\mathsf{p}$, T, $\mathcal{T}_{\mathsf{p},\mathrm{si}}$
Initialization:

$\mathbf{y} \leftarrow \mathbf{y}_\mathsf{p}$, $\mathbf{A} \leftarrow \mathbf{A}_\mathsf{p}$, $\mathcal{T}_\mathrm{si} \leftarrow \mathcal{T}_{\mathsf{p},\mathrm{si}}$
$l \leftarrow 0$, $\mathbf{r}_l \leftarrow \mathbf{y}$, $\hat{\mathcal{T}}_l \leftarrow \emptyset$, $\hat{\mathbf{x}}_l \leftarrow 0$

Iteration:

repeat
  $l \leftarrow l+1$ (Iteration counter)
  $\check{\mathcal{T}}_l \leftarrow \mathsf{supp}(\mathbf{A}^*\mathbf{r}_{l-1}, T)$
  $\tilde{\mathcal{U}}_l \leftarrow \check{\mathcal{T}}_l \cup \hat{\mathcal{T}}_{l-1}$
  $\tilde{\mathbf{x}}_l$ such that $\tilde{\mathbf{x}}_{\tilde{\mathcal{U}}_l} \leftarrow \mathbf{A}^\dagger_{\tilde{\mathcal{U}}_l}\mathbf{y}$; $\tilde{\mathbf{x}}_{\tilde{\mathcal{U}}_l^c} \leftarrow \mathbf{0}$
  $\acute{\mathcal{T}}_l \leftarrow \mathsf{supp}(\tilde{\mathbf{x}}_l, T)$
  $\check{\mathcal{U}}_l \leftarrow \acute{\mathcal{T}}_l \cup \mathcal{T}_\mathrm{si}$
  $\check{\mathbf{x}}_l$ such that $\check{\mathbf{x}}_{\check{\mathcal{U}}_l} \leftarrow \mathbf{A}^\dagger_{\check{\mathcal{U}}_l}\mathbf{y}$; $\check{\mathbf{x}}_{\check{\mathcal{U}}_l{}^c} \leftarrow \mathbf{0}$
  $\hat{\mathcal{T}}_l \leftarrow \mathsf{supp}(\check{\mathbf{x}}_l, T)$
  $\hat{\mathbf{x}}_l$ such that $\hat{\mathbf{x}}_{\hat{\mathcal{T}}_l} \leftarrow \mathbf{A}^\dagger_{\hat{\mathcal{T}}_l}\mathbf{y}$; $\hat{\mathbf{x}}_{\hat{\mathcal{T}}_l^c} \leftarrow \mathbf{0}$
  $\mathbf{r}_l \leftarrow \mathbf{y} - \mathbf{A}\hat{\mathbf{x}}_l$
until *stopping criterion*

Output: $\hat{\mathbf{x}}_\mathsf{p} \leftarrow \hat{\mathbf{x}}_l$, $\hat{\mathcal{T}}_\mathsf{p} \leftarrow \hat{\mathcal{T}}_l$, $\mathbf{r}_\mathsf{p} \leftarrow \mathbf{r}_l$

SIPP algorithm). Based on this, the task of the `consensus` algorithm is to estimate the common support-set as $\hat{\mathcal{J}}_\mathsf{p}$ and the task for the `expansion` is to expand $\hat{\mathcal{J}}_\mathsf{p}$ based on $\hat{\mathcal{T}}_\mathsf{p}$.

Algorithm 2 `consensus`: *Executed in the local node* p

Input: $\{\hat{\mathcal{T}}_\mathsf{q}\}_{\mathsf{q}\in\mathcal{L}_\mathsf{p}^\mathrm{in}}$, $\hat{\mathcal{T}}_\mathsf{p}$, T
Initialization: $\mathbf{z} \leftarrow \mathbf{0}_{N\times 1}$
Algorithm:

$\mathbf{z} \leftarrow \mathtt{vote}_1(\mathbf{z}, \hat{\mathcal{T}}_\mathsf{p})$ (p-th node's estimate)
for each $\mathsf{q} \in \mathcal{L}_\mathsf{p}^\mathrm{in}$ **do**
  $\mathbf{z} \leftarrow \mathtt{vote}_1(\mathbf{z}, \hat{\mathcal{T}}_\mathsf{q})$ (The neigbors' estimates)
end for
Choose $\hat{\mathcal{J}}_\mathsf{p}$ s.t. $(z(i) \geq 2)\ \forall i \in \hat{\mathcal{J}}_\mathsf{p}$ and $|\hat{\mathcal{J}}_\mathsf{p}| \leq T$

Output: $\hat{\mathcal{J}}_\mathsf{p}$

The `consensus` algorithm is described in algorithm 2. The `consensus` strategy is to choose those indices for $\hat{\mathcal{J}}_\mathsf{p}$ that are present in support-sets of at least two incoming neighbor nodes. Our conjecture is that an index present in two nodes' support-set estimates has a high probability of being in the common support $\mathcal{J}$. The conjecture is based on a general acceptance of democratic voting principle. Studying algorithm 2, the inputs are: a set of estimated support-sets $\{\hat{\mathcal{T}}_\mathsf{q}\}_{\mathsf{q}\in\mathcal{L}^\mathrm{in}}$ from the neighbors, the own estimated support-set $\hat{\mathcal{T}}_\mathsf{p}$, and the sparsity level T. The estimate of $\hat{\mathcal{J}}_\mathsf{p}$ is formed (step 5) such that no index in $\hat{\mathcal{J}}_\mathsf{p}$ has less than two votes (i.e., each index in $\hat{\mathcal{J}}_\mathsf{p}$ is present in at least two support-sets from $\{\{\hat{\mathcal{T}}_\mathsf{q}\}_{\mathsf{q}\in\mathcal{L}_\mathsf{p}^\mathrm{in}}, \hat{\mathcal{T}}_\mathsf{p}\}$)[1]. If the number of indices with at least two votes exceed the cardinality T, we pick the T lexicographically.

[1]For node p, this is equivalent to let algorithm choose $\hat{\mathcal{J}}_\mathsf{p}$ as the union of all pair-wise intersections of support-sets (see the analysis section IV-B for details).

Next the `expansion` algorithm is described in algorithm 3 where the task is to expand $\hat{\mathcal{J}}_\mathsf{p}$ to a T-size support $\mathcal{T}_{\mathsf{p},\mathrm{si}}$, which is later used as side information. Note that $\hat{\mathcal{I}}_\mathsf{p} \subset \hat{\mathcal{T}}_\mathsf{p} = \mathsf{supp}(\hat{\mathbf{x}}_\mathsf{p})$ and $\hat{\mathcal{T}}_\mathsf{p} \setminus \hat{\mathcal{I}}_\mathsf{p}$ does not contribute to form $\mathcal{T}_{\mathsf{p},\mathrm{si}}$.

Algorithm 3 `expansion`: *Executed in the local node* p

Input: $\hat{\mathcal{J}}_\mathsf{p}$, $\hat{\mathbf{x}}_\mathsf{p}$, T
Algorithm:

$\hat{\mathbf{x}}_{\mathsf{p},\hat{\mathcal{J}}_\mathsf{p}} \leftarrow \mathbf{0}$
$\hat{\mathcal{I}}_\mathsf{p} \leftarrow \mathsf{supp}(\hat{\mathbf{x}}_\mathsf{p}, T - |\hat{\mathcal{J}}_\mathsf{p}|)$

Output: $\mathcal{T}_{\mathsf{p},\mathrm{si}} \leftarrow \hat{\mathcal{I}}_\mathsf{p} \cup \hat{\mathcal{J}}_\mathsf{p}$ $(|\mathcal{T}_{\mathsf{p},\mathrm{si}}| = T)$

C. DIPP: Distributed Parallel Pursuit

Using algorithm 1, 2 and 3, we now develop the distributed parallel pursuit (DIPP) presented in algorithm 4.

Algorithm 4 Distributed parallel pursuit (DIPP)
Executed in the local node p

Input: $\mathbf{y}_\mathsf{p}$, $\mathbf{A}_\mathsf{p}$, T, $\mathcal{L}_\mathsf{p}^\mathrm{in}$, $\mathcal{L}_\mathsf{p}^\mathrm{out}$
Initialization: $k \leftarrow 0$, $(\hat{\mathbf{x}}_{\mathsf{p},k}, \hat{\mathcal{T}}_{\mathsf{p},k}, \mathbf{r}_{\mathsf{p},k}) \leftarrow \mathrm{SIPP}(\mathbf{y}_\mathsf{p}, \mathbf{A}_\mathsf{p}, T, \emptyset)$
Iteration:

repeat
  $k \leftarrow k+1$ (Iteration counter)
  Transmit: $\hat{\mathcal{T}}_{\mathsf{p},k}$ to all nodes $\mathsf{p} \in \mathcal{L}_\mathsf{p}^\mathrm{out}$
  Receive: $\hat{\mathcal{T}}_{\mathsf{q},k}$ from all nodes $\mathsf{q} \in \mathcal{L}_\mathsf{p}^\mathrm{in}$
  $\hat{\mathcal{J}}_{\mathsf{p},k} \leftarrow \mathtt{consensus}(\{\hat{\mathcal{T}}_{\mathsf{q},k}\}_{\mathsf{q}\in\mathcal{L}_\mathsf{p}^\mathrm{in}}, \hat{\mathcal{T}}_{\mathsf{p},k-1}, T)$
  $\mathcal{T}_{\mathsf{p},\mathrm{si},k} \leftarrow \mathtt{expansion}(\hat{\mathcal{J}}_{\mathsf{p},k}, \hat{\mathbf{x}}_{\mathsf{p},k-1}, T)$
  $(\hat{\mathbf{x}}_{\mathsf{p},k}, \hat{\mathcal{T}}_{\mathsf{p},k}, \mathbf{r}_{\mathsf{p},k}) \leftarrow \mathrm{SIPP}(\mathbf{y}_\mathsf{p}, \mathbf{A}_\mathsf{p}, T, \mathcal{T}_{\mathsf{p},\mathrm{si},k})$
until *stopping criterion*

Output: $\hat{\mathbf{x}}_\mathrm{DIPP} \leftarrow \hat{\mathbf{x}}_{\mathsf{p},k}$, $\hat{\mathcal{T}}_\mathrm{DIPP} \leftarrow \hat{\mathcal{T}}_{\mathsf{p},k}$

Input to algorithm 4 for the p'th node is the measurement signal $\mathbf{y}_\mathsf{p}$, the measurement matrix $\mathbf{A}_\mathsf{p}$, and sparsity T. We assume some underlying communication scheme provides for the transmit and receive functionality. In the initialization phase, an iteration parameter 'k' is set to 0 and the SIPP algorithm is executed with $\mathcal{T}_{\mathsf{p},\mathrm{si}} = \emptyset$.

In the iterations, support-set estimates are exchanged over the network (steps 3 and 4). The `consensus` algorithm produces an estimate of the common support-set $\hat{\mathcal{J}}_{\mathsf{p},k}$ (step 5). Then, the `expansion` (step 6) is used to extend $\hat{\mathcal{J}}_{\mathsf{p},k}$, using $\hat{\mathcal{T}}_{\mathsf{p},k-1}$, to produce $\mathcal{T}_{\mathsf{p},\mathrm{si},k}$. $\mathcal{T}_{\mathsf{p},\mathrm{si},k}$ is then used as an input for the next iteration of SIPP. As *stopping criterion*, we can use an upper limit of iterations and/or violation of non-decreasing residual norm condition (i.e., violation of $\|\mathbf{r}_{\mathsf{p},k}\| \leq \|\mathbf{r}_{\mathsf{p},k-1}\|$).

IV. Distributed Parallel Pursuit: Analysis

In this section we will provide theoretical reconstruction guarantees with corresponding system requirements for the DIPP algorithm. We first analyze SIPP, `consensus` and `expansion` separately, and then provide the analysis for DIPP.

A. Analysis of SIPP

In this section, we will derive the reconstruction guarantee of SIPP. As SIPP is executed in each node p, we drop the index p to avoid a notational clutter. The reconstruction guarantee is presented as a performance bound in proposition 4. To derive the bound, we recursively apply a recurrence inequality which is shown in proposition 3. The recurrence inequality describes the change in reconstruction quality between iteration l and $l-1$. We first introduce following lemmas.

Lemma 2:

$$\|\mathbf{x}_{\hat{\mathcal{T}}_l^{\mathrm{c}}}\| \leq \frac{1+\delta_{3T}}{1-\delta_{3T}}\|\mathbf{x}_{\check{\mathcal{U}}_l^{\mathrm{c}}}\| + \frac{2}{\sqrt{1-\delta_{3T}}}\|\mathbf{e}\|$$

Proof: see appendix B. ∎

Lemma 3:

$$\|\mathbf{x}_{\hat{\mathcal{T}}_l^{\mathrm{c}}}\| \leq \frac{1+\delta_{3T}}{1-\delta_{3T}}\|\mathbf{x}_{\tilde{\mathcal{U}}_l^{\mathrm{c}}}\| + \frac{2}{\sqrt{1-\delta_{3T}}}\|\mathbf{e}\|$$

Proof: By studying algorithm 1, it is clear that the functionality between steps 4 and 6 are the same as between steps 7 and 9. Thus, by replacing $\hat{\mathcal{T}}_l$ with $\check{\mathcal{T}}_l$, $\check{\mathcal{U}}_l$ with $\tilde{\mathcal{U}}_l$ and $\check{\mathbf{x}}_l$ with $\tilde{\mathbf{x}}_l$ in the proof of lemma 2, we arrive at this inequality. ∎

Lemma 4:

$$\|\mathbf{x}_{\tilde{\mathcal{U}}_l^{\mathrm{c}}}\| \leq \frac{2\delta_{3T}}{(1-\delta_{3T})^2}\|\mathbf{x}_{\hat{\mathcal{T}}_{l-1}^{\mathrm{c}}}\| + \frac{2\sqrt{1+\delta_{3T}}}{1-\delta_{3T}}\|\mathbf{e}\|$$

Proof: see appendix C. ∎

Using these lemmas we are now ready to derive the recurrence inequality of SIPP.

Proposition 3 (Recurrence inequality of SIPP):

$$\|\mathbf{x}_{\hat{\mathcal{T}}_l^{\mathrm{c}}}\| \leq a_{\text{SIPP}}\|\mathbf{x}_{\hat{\mathcal{T}}_{l-1}^{\mathrm{c}}}\| + b_{\text{SIPP}}\|\mathbf{x}_{\mathcal{T}_{\text{si}}^{\mathrm{c}}}\| + c_{\text{SIPP}}\|\mathbf{e}\|,$$

where

$$a_{\text{SIPP}} = \frac{\delta_{3T}(1+\delta_{3T})^2}{(1-\delta_{3T})^4}$$
$$b_{\text{SIPP}} = \frac{1+\delta_{3T}}{2(1-\delta_{3T})},$$
$$c_{\text{SIPP}} = \frac{4(1+\delta_{3T}^2)}{(1-\delta_{3T})^3}.$$

Proof: To prove the recurrence inequality of SIPP, we apply inequalities tracing backwards for sub-parts of algorithm 1. We will apply the inequalities in the following order:

1) Steps 9 to 7 by using lemma 2.
2) Steps 7 to 6 by forming a new inequality.
3) Steps 6 to 4 by using lemma 3.
4) Steps 4 (of iteration l) to 9 (of iteration $l-1$) by using lemma 4.

By combining $\|\mathbf{x}_{\check{\mathcal{U}}_l^{\mathrm{c}}}\| \leq \|\mathbf{x}_{\check{\mathcal{T}}_l^{\mathrm{c}}}\|$ and $\|\mathbf{x}_{\check{\mathcal{U}}_l^{\mathrm{c}}}\| \leq \|\mathbf{x}_{\mathcal{T}_{\text{si}}^{\mathrm{c}}}\|$, we can write

$$\|\mathbf{x}_{\check{\mathcal{U}}_l^{\mathrm{c}}}\| \leq \frac{\|\mathbf{x}_{\check{\mathcal{T}}_l^{\mathrm{c}}}\| + \|\mathbf{x}_{\mathcal{T}_{\text{si}}^{\mathrm{c}}}\|}{2}. \tag{11}$$

By using (11) in lemma 2, we get

$$\begin{aligned}\|\mathbf{x}_{\hat{\mathcal{T}}_l^{\mathrm{c}}}\| &\leq \frac{1+\delta_{3T}}{1-\delta_{3T}}\|\mathbf{x}_{\check{\mathcal{U}}_l{}^{\mathrm{c}}}\| + \frac{2}{\sqrt{1-\delta_{3T}}}\|\mathbf{e}\| \\ &\leq \frac{1+\delta_{3T}}{2(1-\delta_{3T})}\|\mathbf{x}_{\check{\mathcal{T}}_l{}^{\mathrm{c}}}\| + \frac{1+\delta_{3T}}{2(1-\delta_{3T})}\|\mathbf{x}_{\mathcal{T}_{\text{si}}^{\mathrm{c}}}\| + \frac{2}{\sqrt{1-\delta_{3T}}}\|\mathbf{e}\|.\end{aligned} \tag{12}$$

We now apply lemma 3 to (12)

$$\begin{aligned}\|\mathbf{x}_{\hat{\mathcal{T}}_l^{\mathrm{c}}}\| &\leq \frac{1+\delta_{3T}}{2(1-\delta_{3T})}\left(\frac{1+\delta_{3T}}{1-\delta_{3T}}\|\mathbf{x}_{\tilde{\mathcal{U}}_l^{\mathrm{c}}}\| + \frac{2}{\sqrt{1-\delta_{3T}}}\|\mathbf{e}\|\right) \\ &\quad + \frac{1+\delta_{3T}}{2(1-\delta_{3T})}\|\mathbf{x}_{\mathcal{T}_{\text{si}}^{\mathrm{c}}}\| + \frac{2}{\sqrt{1-\delta_{3T}}}\|\mathbf{e}\| \\ &\overset{(a)}{\leq} \frac{(1+\delta_{3T})^2}{2(1-\delta_{3T})^2}\|\mathbf{x}_{\tilde{\mathcal{U}}_l^{\mathrm{c}}}\| + \frac{1+\delta_{3T}}{2(1-\delta_{3T})}\|\mathbf{x}_{\mathcal{T}_{\text{si}}^{\mathrm{c}}}\| + \frac{3-\delta_{3T}}{(1-\delta_{3T})^2}\|\mathbf{e}\|.\end{aligned} \tag{13}$$

Here, we have in (a) used that $1-\delta_{3T} \leq \sqrt{1-\delta_{3T}}$. To finalize the bound we apply lemma 4 to (13)

$$\begin{aligned}\|\mathbf{x}_{\hat{\mathcal{T}}_l^{\mathrm{c}}}\| &\leq \frac{(1+\delta_{3T})^2}{2(1-\delta_{3T})^2}\left(\frac{2\delta_{3T}}{(1-\delta_{3T})^2}\|\mathbf{x}_{\hat{\mathcal{T}}_{l-1}^{\mathrm{c}}}\| + \frac{2\sqrt{1+\delta_{3T}}}{1-\delta_{3T}}\|\mathbf{e}\|\right) \\ &\quad + \frac{1+\delta_{3T}}{2(1-\delta_{3T})}\|\mathbf{x}_{\mathcal{T}_{\text{si}}^{\mathrm{c}}}\| + \frac{3-\delta_{3T}}{(1-\delta_{3T})^2}\|\mathbf{e}\| \\ &\overset{(a)}{\leq} \frac{\delta_{3T}(1+\delta_{3T})^2}{2(1-\delta_{3T})^4}\|\mathbf{x}_{\hat{\mathcal{T}}_{l-1}^{\mathrm{c}}}\| + \frac{1+\delta_{3T}}{2(1-\delta_{3T})}\|\mathbf{x}_{\mathcal{T}_{\text{si}}^{\mathrm{c}}}\| + \frac{4(1+\delta_{3T}^2)}{(1-\delta_{3T})^3}\|\mathbf{e}\|.\end{aligned}$$

In (a) we have used for the noise-term that $\frac{(1+\delta_{3T})^2}{2(1-\delta_{3T})^2}\frac{2\sqrt{1+\delta_{3T}}}{1-\delta_{3T}} + \frac{3-\delta_{3T}}{(1-\delta_{3T})^2} \leq \frac{(1+\delta_{3T})^3}{(1-\delta_{3T})^3} + \frac{3-\delta_{3T}}{(1-\delta_{3T})^2} = \frac{4-\delta_{3T}+4\delta_{3T}^2+\delta_{3T}^3}{(1-\delta_{3T})^3} \leq \frac{4(1+\delta_{3T}^2)}{(1-\delta_{3T})^3}$. This concludes the proof. ∎

By using a fixed iteration counter, we use the recurrence inequality in proposition 3 to provide the following reconstruction performance bound.

Proposition 4 (Performance bound of SIPP): If $a_{\text{SIPP}} < 1$, then after $l^* = \left\lceil \log\left(\frac{\|\mathbf{e}\|}{\|\mathbf{x}\|}\right) / \log\left(a_{\text{SIPP}}\right) \right\rceil$ iterations, the performance of the SIPP algorithm is bounded by

$$\|\mathbf{x}_{\hat{\mathcal{T}}_{\text{SIPP}}^{\mathrm{c}}}\| \leq \frac{b_{\text{SIPP}}}{1-a_{\text{SIPP}}}\|\mathbf{x}_{\mathcal{T}_{\text{si}}^{\mathrm{c}}}\| + \frac{1-a_{\text{SIPP}}+c_{\text{SIPP}}}{1-a_{\text{SIPP}}}\|\mathbf{e}\|, \tag{14}$$

or

$$\begin{aligned}\|\mathbf{x}-\hat{\mathbf{x}}_{\text{SIPP}}\| &\leq \frac{b_{\text{SIPP}}}{(1-\delta_{3T})(1-a_{\text{SIPP}})}\|\mathbf{x}_{\mathcal{T}_{\text{si}}^{\mathrm{c}}}\| \\ &\quad + \left(\frac{1-a_{\text{SIPP}}+c_{\text{SIPP}}}{(1-\delta_{3T})(1-a_{\text{SIPP}})} + \frac{1}{\sqrt{1-\delta_{3T}}}\right)\|\mathbf{e}\|\end{aligned} \tag{15}$$

where a_{SIPP}, b_{SIPP} and c_{SIPP} are defined in proposition 3, $\hat{\mathbf{x}}_{\text{SIPP}}$ and $\hat{\mathcal{T}}_{\text{SIPP}}$ are outputs of algorithm 1.

Proof: We start with proving (14). We do this by iteratively applying proposition 3 two times:

$$\begin{aligned}\|\mathbf{x}_{\hat{\mathcal{T}}_l^{\mathrm{c}}}\| &\leq a_{\text{SIPP}}\|\mathbf{x}_{\hat{\mathcal{T}}_{l-1}^{\mathrm{c}}}\| + b_{\text{SIPP}}\|\mathbf{x}_{\mathcal{T}_{\text{si}}^{\mathrm{c}}}\| + c_{\text{SIPP}}\|\mathbf{e}\| \\ &\leq a_{\text{SIPP}}\left(a_{\text{SIPP}}\|\mathbf{x}_{\hat{\mathcal{T}}_{l-2}^{\mathrm{c}}}\| + b_{\text{SIPP}}\|\mathbf{x}_{\mathcal{T}_{\text{si}}^{\mathrm{c}}}\| + c_{\text{SIPP}}\|\mathbf{e}\|\right) \\ &\quad + b_{\text{SIPP}}\|\mathbf{x}_{\mathcal{T}_{\text{si}}^{\mathrm{c}}}\| + c_{\text{SIPP}}\|\mathbf{e}\|.\end{aligned}$$

To find a bound of the final performance, we let the iterations

run to l^*

$$\|\mathbf{x}_{\hat{\mathcal{T}}_{\text{SIPP}}^{\text{c}}}\| \leq a_{\text{SIPP}}^{l^*}\|\mathbf{x}_{\hat{\mathcal{T}}_{l-l^*}^{c}}\| + b_{\text{SIPP}}\sum_{i=0}^{l^*-1}a_{\text{SIPP}}^{i}\|\mathbf{x}_{\mathcal{T}_{\text{si}}^{\text{c}}}\| + c_{\text{SIPP}}\sum_{i=0}^{l^*-1}a_{\text{SIPP}}^{i}\|\mathbf{e}\|$$
$$\overset{(a)}{\leq} a_{\text{SIPP}}^{l^*}\|\mathbf{x}\| + \frac{b_{\text{SIPP}}}{1-a_{\text{SIPP}}}\|\mathbf{x}_{\mathcal{T}_{\text{si}}^{\text{c}}}\| + \frac{c_{\text{SIPP}}}{1-a_{\text{SIPP}}}\|\mathbf{e}\|$$
$$\overset{(b)}{=} a_{\text{SIPP}}^{\left\lceil \log\left(\frac{\|\mathbf{e}\|}{\|\mathbf{x}\|}\right)/\log(a_{\text{SIPP}})\right\rceil}\|\mathbf{x}\| + \frac{b_{\text{SIPP}}}{1-a_{\text{SIPP}}}\|\mathbf{x}_{\mathcal{T}_{\text{si}}^{\text{c}}}\| + \frac{c_{\text{SIPP}}}{1-a_{\text{SIPP}}}\|\mathbf{e}\|$$
$$\leq \frac{\|\mathbf{e}\|}{\|\mathbf{x}\|}\|\mathbf{x}\| + \frac{b_{\text{SIPP}}}{1-a_{\text{SIPP}}}\|\mathbf{x}_{\mathcal{T}_{\text{si}}^{\text{c}}}\| + \frac{c_{\text{SIPP}}}{1-a_{\text{SIPP}}}\|\mathbf{e}\|$$
$$= \frac{b_{\text{SIPP}}}{1-a_{\text{SIPP}}}\|\mathbf{x}_{\mathcal{T}_{\text{si}}^{\text{c}}}\| + \frac{1-a_{\text{SIPP}}+c_{\text{SIPP}}}{1-a_{\text{SIPP}}}\|\mathbf{e}\|.$$

In (a) we have used that $a_{\text{SIPP}} < 1$ and the fact that $\|\mathbf{x}_{\hat{\mathcal{T}}_{l^*}^{\text{c}}}\| \leq \|\mathbf{x}\|$. In (b) we insert $l^* = \left\lceil \log\left(\frac{\|\mathbf{e}\|}{\|\mathbf{x}\|}\right)/\log\left(a_{\text{SIPP}}\right)\right\rceil$ from the proposition. The SIPP algorithm use the least squares solution to find $\hat{\mathbf{x}}_{\text{SIPP}}$. Therefore, to get (15) we apply lemma 1 to (14).

$$\|\mathbf{x}-\hat{\mathbf{x}}_{\text{SIPP}}\| \leq \frac{1}{1-\delta_{3T}}\|\mathbf{x}_{\hat{\mathcal{T}}_{\text{SIPP}}^{\text{c}}}\| + \frac{1}{\sqrt{1-\delta_{3T}}}\|\mathbf{e}\|$$
$$\leq \frac{1}{1-\delta_{3T}}\left(\frac{b_{\text{SIPP}}}{1-a_{\text{SIPP}}}\|\mathbf{x}_{\mathcal{T}_{\text{si}}^{\text{c}}}\| + \frac{1-a_{\text{SIPP}}+c_{\text{SIPP}}}{1-a_{\text{SIPP}}}\|\mathbf{e}\|\right) + \frac{1}{\sqrt{1-\delta_{3T}}}\|\mathbf{e}\|$$
$$= \frac{b_{\text{SIPP}}}{(1-\delta_{3T})(1-a_{\text{SIPP}})}\|\mathbf{x}_{\mathcal{T}_{\text{si}}^{\text{c}}}\| + \left(\frac{1-a_{\text{SIPP}}+c_{\text{SIPP}}}{(1-\delta_{3T})(1-a_{\text{SIPP}})} + \frac{1}{\sqrt{1-\delta_{3T}}}\right)\|\mathbf{e}\|.$$

■

Corollary 2: The SIPP algorithm reaches a solution independent of the realization of $\mathbf{x}_{\hat{\mathcal{T}}}$ if and only if

$$\delta_{3T} \leq r,$$

where r is the solution to $a_{\text{SIPP}} = 1$ for $0 < \delta_{3T} < 1$.

Proof: For the SIPP algorithm to converge, it is required that $a_{\text{SIPP}} < 1$. We also know that $0 < \delta_{3T} < 1$. We thus solve:

$$\begin{aligned}
& a_{\text{SIPP}} = 1 \\
\Leftrightarrow \quad & \frac{\delta_{3T}(1+\delta_{3T})^2}{(1-\delta_{3T})^4} = 1 \\
\Leftrightarrow \quad & \delta_{3T}(1+\delta_{3T})^2 = (1-\delta_{3T})^4 \\
\Leftrightarrow \quad & \delta_{3T} + 2\delta_{3T}^2 + \delta_{3T}^3 = 1 - 4\delta_{3T} + 6\delta_{3T}^2 - 4\delta_{3T}^3 + \delta_{3T}^4 \\
\Leftrightarrow \quad & 0 = 1 - 5\delta_{3T} + 4\delta_{3T}^2 - 5\delta_{3T}^3 + \delta_{3T}^4.
\end{aligned}$$

This gives solutions

$$\delta_{3T,1} = 4.33..., \quad \delta_{3T,2} = 0.219... + i0.976...,$$
$$\delta_{3T,3} = 0.231..., \quad \delta_{3T,4} = 0.219... - i0.976...,$$

where the only solution r that lies in the interval of δ_{3T} is $r = \delta_{3T,3}$. ■

Example 1: In this example , if we have $\delta_{3T} = 0.17$, we get $a_{\text{SIPP}} < 0.50$, $b_{\text{SIPP}} < 0.71$, $c_{\text{SIPP}} < 7.20$. Then according to proposition 4, after $l^* = \left\lceil \log\left(\frac{\|\mathbf{e}\|}{\|\mathbf{x}\|}\right)/\log\left(0.5\right)\right\rceil$ iterations the performance of SIPP fulfills the following bounds

$$\|\mathbf{x}_{\hat{\mathcal{T}}_{\text{SIPP}}^{\text{c}}}\| < 1.42\|\mathbf{x}_{\mathcal{T}_{\text{si}}^{\text{c}}}\| + 15.2\|\mathbf{e}\|,$$

or

$$\|\mathbf{x}-\hat{\mathbf{x}}_{\text{SIPP}}\| < 1.72\|\mathbf{x}_{\mathcal{T}_{\text{si}}^{\text{c}}}\| + 19.4\|\mathbf{e}\|.$$

By this example we see that SIPP reaches its performance bound when $\delta_{3T} \leq 0.17$ whereas SP requires $\delta_{3T} \leq 0.139$ [36] for a similar result.

Example 2: If we instead have that $\delta_{3T} = 0.23$, we get that after $l^* = \left\lceil \log\left(\frac{\|\mathbf{e}\|}{\|\mathbf{x}\|}\right)/\log\left(0.99\right)\right\rceil$ iterations the performance of SIPP fulfills the following bounds

$$\|\mathbf{x}_{\hat{\mathcal{T}}_{\text{SIPP}}^{\text{c}}}\| < 78.8\|\mathbf{x}_{\mathcal{T}_{\text{si}}^{\text{c}}}\| + 912\|\mathbf{e}\|,$$

or

$$\|\mathbf{x}-\hat{\mathbf{x}}_{\text{SIPP}}\| < 95.4\|\mathbf{x}_{\mathcal{T}_{\text{si}}^{\text{c}}}\| + 1.19\cdot 10^3\|\mathbf{e}\|.$$

This example provides the ultimate bound, for larger δ_{3T} we cannot guarantee any bound.

B. Analysis of fusion

Fusion has two parts: `consensus` and `expansion`. The strategy of `consensus` is based on a voting principle, which in general is non-trivial to analyze due to the counting of non-negative integers followed by decision. The `consensus` endeavors to estimate the joint support part for sensor node p as $\hat{\mathcal{J}}_{\mathsf{p}}$. Following algorithm 2, we note that

$$\hat{\mathcal{J}}_{\mathsf{p}} = \left\{i : i \in \left((\hat{\mathcal{T}}_{\mathsf{p}} \cap \hat{\mathcal{T}}_{\mathsf{q}}) \cup (\hat{\mathcal{T}}_{\mathsf{q}} \cap \hat{\mathcal{T}}_{\mathsf{r}})\right),\ \forall \mathsf{q},\mathsf{r} \in \mathcal{L}_{\mathsf{p}}^{\text{in}}, \mathsf{q} \neq \mathsf{r}\right\}$$

Any index $i \in \mathcal{T}_{\mathsf{p}}$ is referred to as a correct index for node p. Let us denote the probability of an index from the output of the SIPP algorithm $i \in \hat{\mathcal{T}}_{\mathsf{p}}$ to be correct by the probability: $\mathbb{P}\big(i \in \mathcal{T}_{\mathsf{p}} | i \in \hat{\mathcal{T}}_{\mathsf{p}}\big)$, and the probability of index $i \in \hat{\mathcal{J}}_{\mathsf{p}}$ to be correct by the probability: $\mathbb{P}\big(i \in \mathcal{T}_{\mathsf{p}} | i \in \hat{\mathcal{J}}_{\mathsf{p}}\big)$. Using the voting principle, we apply the following assumption.

Assumption 2: $\hat{\mathcal{J}}_{\mathsf{p}}$ is at-least as reliable as $\hat{\mathcal{T}}_{\mathsf{p}}$ in a probabilistic sense. That is

$$\mathbb{P}\big(i \in \mathcal{T}_{\mathsf{p}} | i \in \hat{\mathcal{J}}_{\mathsf{p}}\big) \geq \mathbb{P}\big(i \in \mathcal{T}_{\mathsf{p}} | i \in \hat{\mathcal{T}}_{\mathsf{p}}\big),$$

where $\mathbb{P}(\cdot)$ denotes the probability. □

Following algorithm 3, `expansion` provides an estimate of $\mathcal{T}_{\mathsf{p}}$ as $\mathcal{T}_{\mathsf{p,si}} = \hat{\mathcal{I}}_{\mathsf{p}} \cup \hat{\mathcal{J}}_{\mathsf{p}}$, where inclusion of $\hat{\mathcal{J}}_{\mathsf{p}}$ is motivated by assumption 2. To maintain the cardinality of $|\mathcal{T}_{\mathsf{p,si}}| = T$, the `expansion` algorithm discards $\hat{\mathcal{T}}_{\mathsf{p}} \setminus \hat{\mathcal{I}}_{\mathsf{p}}$. Naturally we bring the following assumption.

Assumption 3: Signal coefficients associated with $\hat{\mathcal{J}}_{\mathsf{p}}$ contains at-least as much energy than the signal coefficients associated with the discarded $\hat{\mathcal{T}}_{\mathsf{p}} \setminus \hat{\mathcal{I}}_{\mathsf{p}}$. That is

$$\|(\mathbf{x}_{\mathsf{p}})_{\hat{\mathcal{J}}_{\mathsf{p}}}\|^2 \geq \|(\mathbf{x}_{\mathsf{p}})_{\hat{\mathcal{T}}_{\mathsf{p}} \setminus \hat{\mathcal{I}}_{\mathsf{p}}}\|^2.$$

□

Using assumption 3, we will in proposition 5 characterize the performance bound of the `expansion` algorithm. First, we introduce the following lemma.

Lemma 5:

$$\|(\mathbf{x}_{\mathsf{p}})_{\mathcal{T}_{\mathsf{p,si}}^{\text{c}}}\|^2 = \|(\mathbf{x}_{\mathsf{p}})_{\hat{\mathcal{T}}_{\mathsf{p}}^{\text{c}}}\|^2 + \|(\mathbf{x}_{\mathsf{p}})_{\hat{\mathcal{T}}_{\mathsf{p}} \setminus \hat{\mathcal{I}}_{\mathsf{p}}}\|^2 - \|(\mathbf{x}_{\mathsf{p}})_{\hat{\mathcal{J}}_{\mathsf{p}}}\|^2$$

Proof: In the proof, we drop notation p. We have that $\hat{\mathcal{I}} \subseteq \hat{\mathcal{T}}$ and $\hat{\mathcal{I}} \subseteq \mathcal{T}_{\text{si}}$ by construction and definition, respectively. For the initial support-set we have that:

$$\begin{aligned}\|\mathbf{x}_{\mathcal{T}_{\text{si}}^{\text{c}}}\|^2 &= \|\mathbf{x}_{(\hat{\mathcal{I}}\cup\hat{\mathcal{J}})^{\text{c}}}\|^2 \\ &\overset{(a)}{=} \|\mathbf{x}_{\hat{\mathcal{I}}^{\text{c}}\cap\hat{\mathcal{J}}^{\text{c}}}\|^2 \\ &= \|\mathbf{x}_{\hat{\mathcal{I}}^{\text{c}}\setminus\hat{\mathcal{J}}}\|^2 \\ &\overset{(b)}{=} \|\mathbf{x}_{\hat{\mathcal{I}}^{\text{c}}}\|^2 - \|\mathbf{x}_{\hat{\mathcal{J}}}\|^2. \end{aligned} \tag{21}$$

In (a) we have used De Morgan's law and in (b) we have used that $\hat{\mathcal{J}} \subset \hat{\mathcal{I}}^{\text{c}}$. By the same trick we also have that

$$\|\mathbf{x}_{\hat{\mathcal{T}}^{\text{c}}}\|^2 = \|\mathbf{x}_{\hat{\mathcal{I}}^{\text{c}}}\|^2 - \|\mathbf{x}_{\hat{\mathcal{T}}\setminus\hat{\mathcal{I}}}\|^2 \tag{22}$$

Putting (22) into (21), we get

$$\begin{aligned}\|\mathbf{x}_{\mathcal{T}_{\text{si}}^{\text{c}}}\|^2 &= \|\mathbf{x}_{\hat{\mathcal{I}}^{\text{c}}}\|^2 - \|\mathbf{x}_{\hat{\mathcal{J}}}\|^2 \\ &= \|\mathbf{x}_{\hat{\mathcal{T}}^{\text{c}}}\|^2 + \|\mathbf{x}_{\hat{\mathcal{T}}\setminus\hat{\mathcal{I}}}\|^2 - \|\mathbf{x}_{\hat{\mathcal{J}}}\|^2.\end{aligned}$$

■

Proposition 5 (Performance bound for expansion):

$$\|(\mathbf{x}_{\text{p}})_{\mathcal{T}_{\text{p,si}}^{\text{c}}}\| \leq a_{\text{co}}\|(\mathbf{x}_{\text{p}})_{\hat{\mathcal{T}}_{\text{p}}^{\text{c}}}\|,$$

where

$$a_{\text{co}} \leq 1.$$

Proof: In the proof, we drop notation p.

$$\begin{aligned}\|\mathbf{x}_{\mathcal{T}_{\text{si}}^{\text{c}}}\| &\overset{(a)}{=} \sqrt{\|\mathbf{x}_{\hat{\mathcal{T}}^{\text{c}}}\|^2 + \|\mathbf{x}_{\hat{\mathcal{T}}\setminus\hat{\mathcal{I}}}\|^2 - \|\mathbf{x}_{\hat{\mathcal{J}}}\|^2} \\ &\overset{(b)}{\leq} \sqrt{\|\mathbf{x}_{\hat{\mathcal{T}}^{\text{c}}}\|^2} = \|\mathbf{x}_{\hat{\mathcal{T}}^{\text{c}}}\| \end{aligned} \tag{23}$$

In (a), we applied lemma 5 and in (b), we used assumption 3. Based on this argument, we introduce the constant $a_{\text{co}} \leq 1$ such that

$$\|\mathbf{x}_{\mathcal{T}_{\text{si}}^{\text{c}}}\| \leq a_{\text{co}}\|\mathbf{x}_{\hat{\mathcal{T}}^{\text{c}}}\| \leq \|\mathbf{x}_{\hat{\mathcal{T}}^{\text{c}}}\|. \tag{24}$$

When the network is good, meaning that the inequality in (23) is large, then a_{co} is small and vice versa. ■

C. Distributed Parallel Pursuit

Now we will characterize a performance bound for DIPP. In order to do so, we first derive the recurrence inequality of DIPP by using the performance bounds of SIPP and `consensus` algorithms.

Proposition 6 (Recurrence inequality of DIPP*):* When $a_{\text{SIPP}} < 1$, the recurrence inequality of DIPP is:

$$\|\mathbf{x}_{\hat{\mathcal{T}}_{\text{p},k}^{\text{c}}}\| < \frac{a_{\text{co}}b_{\text{SIPP}}}{1-a_{\text{SIPP}}}\|\mathbf{x}_{\hat{\mathcal{T}}_{\text{p},k-1}^{\text{c}}}\| + \frac{1-a_{\text{SIPP}}+c_{\text{SIPP}}}{1-a_{\text{SIPP}}}\|\mathbf{e}_{\text{p}}\|,$$

where a_{SIPP}, b_{SIPP}, c_{SIPP} are parameters associated with the underlying SIPP algorithm and a_{co} is a parameter associated with the network, `consensus` and `expansion` algorithm. They are defined as:

$$\begin{aligned}a_{\text{SIPP}} &= \frac{\delta_{3T}(1+\delta_{3T})^2}{(1-\delta_{3T})^4} \\ b_{\text{SIPP}} &= \frac{1+\delta_{3T}}{2(1-\delta_{3T})}, \\ c_{\text{SIPP}} &= \frac{4(1+\delta_{3T})}{(1-\delta_{3T})^3}, \\ a_{\text{co}} &\leq 1.\end{aligned}$$

Proof: Proof in appendix D. ■

Using the recurrence inequality, we can now derive the performance bound of DIPP.

Proposition 7 (Performance bound of DIPP*):* If $a_{\text{SIPP}} < 1$ and $a_{\text{co}}\frac{b_{\text{SIPP}}}{1-a_{\text{SIPP}}} < 1$, then after $k^* = \left\lceil \log\left(\frac{\|\mathbf{e}_{\text{p}}\|}{\|\mathbf{x}\|}\right) / \log\left(a_{\text{co}}\frac{b_{\text{SIPP}}}{1-a_{\text{SIPP}}}\right)\right\rceil$ iterations, the performance of the DIPP algorithm is bounded by:

$$\|(\mathbf{x}_{\text{p}})_{\hat{\mathcal{T}}_{\text{p,DIPP}}^{\text{c}}}\| \leq \left(1 + \frac{1-a_{\text{SIPP}}+c_{\text{SIPP}}}{(1-a_{\text{SIPP}})(1-a_{\text{co}}b_{\text{SIPP}})}\right)\|\mathbf{e}_{\text{p}}\| \tag{25}$$

or

$$\begin{aligned}\|\mathbf{x}_{\text{p}} - \hat{\mathbf{x}}_{\text{p,DIPP}}\| \leq \Big(&\frac{1-a_{\text{SIPP}}+c_{\text{SIPP}}}{(1-\delta_{3T})(1-a_{\text{SIPP}})(1-a_{\text{co}}b_{\text{SIPP}})} \\ &+\frac{2}{1-\delta_{3T}}\Big)\|\mathbf{e}_{\text{p}}\|\end{aligned} \tag{26}$$

where the constants are defined in Proposition 6.

Proof: Proof in appendix D. ■

Example 3: Using $\delta_{3T} = 0.17$ as in Example 1 and $a_{\text{co}} = 0.27$ gives that $a_{\text{SIPP}} < 0.5$ and $a_{\text{co}}\frac{b_{\text{SIPP}}}{1-a_{\text{SIPP}}} < 0.5$. This translates into the following bounds

$$\|(\mathbf{x}_{\text{p}})_{\hat{\mathcal{T}}_{\text{p,DIPP}}^{\text{c}}}\| < 21.7\|\mathbf{e}_{\text{p}}\|,$$

or,

$$\|\mathbf{x}_{\text{p}} - \hat{\mathbf{x}}_{\text{p,DIPP}}\| < 27.4\|\mathbf{e}_{\text{p}}\|.$$

Example 4: Using $\delta_{3T} = 0.23$ as in Example 2 and $a_{\text{co}} = 1.61 \cdot 10^{-4}$ gives that $a_{\text{SIPP}} < 0.99$ and $a_{\text{co}}\frac{b_{\text{SIPP}}}{1-a_{\text{SIPP}}} < 1$. This translates into the following bounds

$$\|(\mathbf{x}_{\text{p}})_{\hat{\mathcal{T}}_{\text{p,DIPP}}^{\text{c}}}\| < 9.12 \cdot 10^2\|\mathbf{e}_{\text{p}}\|,$$

or,

$$\|\mathbf{x}_{\text{p}} - \hat{\mathbf{x}}_{\text{p,DIPP}}\| < 1.19 \cdot 10^3\|\mathbf{e}_{\text{p}}\|.$$

In the DIPP algorithm, there are two parameters that impact the performance. The classical RIC δ_{3T}, and the performance of the `consensus` and `expansion` algorithms expressed in a_{co}. If both of these are good (small δ_{3T} and a_{co}), then the algorithm will perform well. One main advantage of the DIPP algorithm compared to a standard, disconnected, algorithm is that we can allow δ_{3T} to be bigger than in a single-node case while still providing a bound independent of signal realization, provided that a_{co} is then smaller.

V. Simulation Results

We have provided several analytical performance bounds for DIPP and the underlying sub-algorithms. These bounds put restrictions on the system in terms of RIC (δ_T) and network connectivity (a_{co}). In practice, it turns out that reconstruction algorithms for CS usually perform well at significantly less restrictive set-ups. We use a non-decreasing norm stopping criterion in our algorithm.

A. Performance Measures and Experimental Setups

We use two performance measures. The first performance measure is called signal-to-reconstruction-error ratio (SRER), defined as

$$\text{SRER} = \frac{\mathcal{E}\{\|\mathbf{x}\|_2^2\}}{\mathcal{E}\{\|\mathbf{x}-\hat{\mathbf{x}}\|_2^2\}},$$

where $\mathcal{E}$ is the expectation taken over all nodes and all realizations. Our objective is to achieve a higher SRER. Note that the SRER is the inverse of normalized mean square error.

We also define a measure which provides a direct evaluation of the support-set recovery performance. This is a distortion measure $d(\mathcal{T},\hat{\mathcal{T}}) = 1 - \left(|\mathcal{T}\cap\hat{\mathcal{T}}|/|\mathcal{T}|\right)$ [37], which we recently used in [11]. Here, $\mathcal{T}_{\mathsf{p}}$ is the local support-set, that is $\mathcal{T}_{\mathsf{p}} = \mathcal{J}\cup\mathcal{I}_{\mathsf{p}}$. Considering a large number of realizations, we can compute the average of $d(\mathcal{T}_{\mathsf{p}},\hat{\mathcal{T}}_{\mathsf{p}})$. Based on this distortion, we define the average support-set cardinality error (ASCE) as follows

$$\text{ASCE} = \mathcal{E}\left\{d(\mathcal{T},\hat{\mathcal{T}})\right\} = 1 - \mathcal{E}\left\{\frac{|\mathcal{T}\cap\hat{\mathcal{T}}|}{|\mathcal{T}|}\right\}.$$

Note that the ASCE has the range $[0,1]$ and our objective is to achieve a lower ASCE. Along-with SRER, the ASCE is used as the second performance evaluation measure because the principle of greedy algorithms is to estimate the underlying support-set. We perform average based empirical testing, where SRER and ASCE are computed for large sets of data. To measure the level of under-sampling, we define the fraction of measurements

$$\alpha = \frac{M}{N}.$$

For a given network topology $\mathbf{C}_i$, $i \in [0, |\mathcal{L}|-1]$ (see section II-C), the steps of testing strategy are listed as follows:

1) Given the parameters N, T choose an α (such that M is an integer).
2) Randomly generate a set of $M \times N$ sensing matrices $\{\mathbf{A}_{\mathsf{p}}\}_{\mathsf{p}=1}^{|\mathcal{L}|}$ where the components are drawn independently from an i.i.d. Gaussian source (i.e. $a_{k,l} \sim \mathcal{N}\left(0, \frac{1}{M}\right)$) and then scale the columns of $\mathbf{A}_{\mathsf{p}}$ to unit-norm.
3) Randomly generate a set of signal vectors $\{\mathbf{x}_{\mathsf{p}}\}_{l=p}^{|\mathcal{L}|}$ following Section II-B. The common and private support-sets are chosen uniformly over the set $\{1,2,\ldots,N\}$. The non-zero components of $\mathbf{x}_{\mathsf{p}}$ are independently drawn by either of the following two methods.
   a) The non-zero components are drawn independently from a standard Gaussian source. This type of signal is referred to as Gaussian sparse signal.
   b) The non-zero components are set to ones. This type of signal is referred to as binary sparse signal.

   Note that the Gaussian sparse signal is compressible in nature, meaning that, in the descending order, the sorted amplitudes of a Gaussian sparse signal vector's components decay fast with respect to the sorted indices. This decaying trend corroborates with several natural signals (for example, wavelet coefficients of an image). On the other hand, a binary sparse signal is not compressible in nature, but of special interest for comparative study, since it represents a particularly challenging case for greedy reconstruction strategies [9], [15].
4) Compute the measurements $\mathbf{y}_{\mathsf{p}} = \mathbf{A}_{\mathsf{p}}\mathbf{x}_{\mathsf{p}} + \mathbf{e}_{\mathsf{p}}, \forall \mathsf{p} \in \mathcal{L}$. Here $\mathbf{e}_{\mathsf{p}} \sim \mathcal{N}(\mathbf{0}, \sigma_e^2\mathbf{I}_M)$.
5) Apply the CS algorithms on the data $\{\mathbf{y}_{\mathsf{p}}\}_{\mathsf{p}=1}^{|\mathcal{L}|}$ independently.

In the above simulation procedure, for each node $\mathsf{p} \in \mathcal{L}$, 10^2 realizations of sensing matrices were used, and, for each sensing node, 10^2 realizations of data vectors were used. We used 10 nodes in the network. Thus, the performance is averaged over $10 \cdot 100 \cdot 100 = 10^5$ data.

Considering the measurement noise $\mathbf{e}_{\mathsf{p}} \sim \mathcal{N}\left(\mathbf{0}, \sigma_e^2\mathbf{I}_M\right)$, we define the signal-to-measurement-noise-ratio (SMNR) as

$$\text{SMNR} = \frac{\mathcal{E}\{\|\mathbf{x}_{\mathsf{p}}\|_2^2\}}{\mathcal{E}\{\|\mathbf{e}_{\mathsf{p}}\|_2^2\}},$$

where $\mathcal{E}\{\|\mathbf{e}_{\mathsf{p}}\|_2^2\} = \sigma_e^2 M$. For noisy measurement case, we report the experimental results at SMNR 20 dB.

In the convergence and performance results we have used the signal dimensionality $N = 1000$, $J = 15$ and $I_{\mathsf{p}} = 5$, giving $T = 20$. Such a 2% sparsity level is chosen in accordance with real life scenarios, for example most of the energy of an image signal in the wavelet domain is concentrated within $2-4\%$ coefficients [38].

B. Performance Results

We now provide the average performance results using the performance measures SRER and ASCE described earlier. We report the results in three subsections, first we present the results for noisy binary signals, secondly for noisy Gaussian signals and lastly for clean Gaussian signals. The performance of SP is included as a benchmark performance because DIPP is based on SIPP which is a modification of SP.

1) Binary signals with additive noise: In Fig. 3 we provide performance results for DIPP using binary sparse signals with SMNR $= 20$ dB. We note that the performance of the system improves significantly as the connectivity in the network improves (remember that a_{co} is the network parameter). Similarly, we see improvement in the system with growing α because a growing α improves the RIC δ_T parameter. Observe that ASCE tends to zero as α increases which means that there will in average be no support-set errors after some point.

2) Gaussian signals with additive noise: In Fig. 4 we present the results for Gaussian sparse signals under SMNR $=$ 20 dB. Here also we notice significant performance improvement. For example, in Fig. 4b, at $\alpha = 0.16$, DIPP in a network of 4 neighbors provides almost 13 dB performance gain over

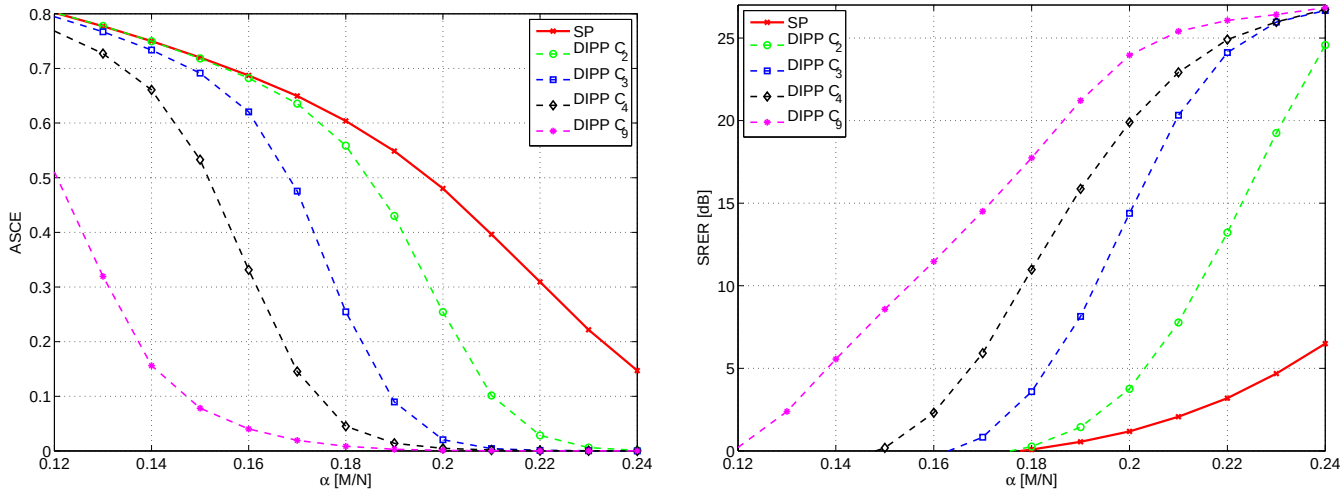

(a) ASCE vs fraction of measurements (b) SRER vs fraction of measurements

Fig. 3. Reconstruction of binary sparse signals at SMNR = 20 dB, by varying network connectivity and fraction of measurements α.

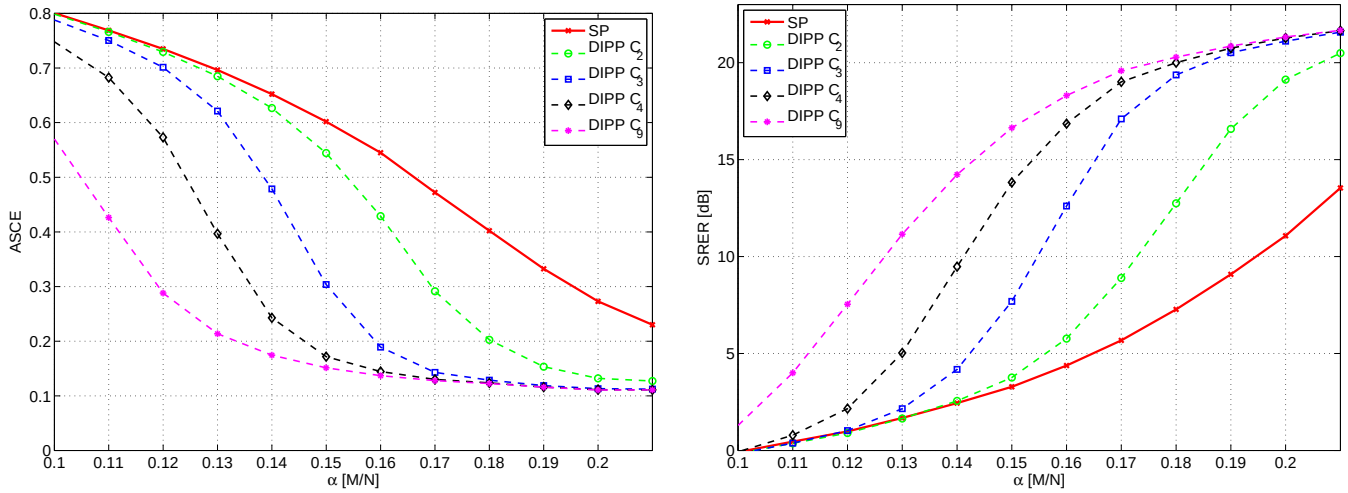

(a) ASCE vs fraction of measurements (b) SRER vs fraction of measurements

Fig. 4. Reconstruction of Gaussian sparse signals at SMNR = 20 dB, by varying network connectivity and fraction of measurements α.

SP. As we expect, the ASCE never reaches 0 since in a local node, strong noise may be mistaken for signal components.

3) Gaussian signals in clean condition: Finally Fig. 5 shows performance for Gaussian sparse signals in clean environment (no measurement noise). Here, we are expected to achieve perfect signal recovery for better system conditions, such as a higher α and/or a higher network connectivity. Therefore, the SRER may theoretically reach ∞ which in our case will be at the level of machine precision. In such case, the ASCE may provide a better reference curve since it tends to zero rather than ∞. We found that such perfect reconstruction quality can be achieved by increasing network connectivity at a fixed α.

Reproducible results: In the spirit of reproducible results, we provide a package with all necessary MATLAB codes in the following website: http://www.ee.kth.se/ctsoftware. In this package consult the README.TXT file to obtain instructions on how to reproduce the figures presented in this paper.

VI. Conclusions

We show the viability of designing greedy pursuit algorithms for distributed compressed sensing with provable theoretical guarantees based on appropriate assumptions about signal models, sensors and connection networks, as well as providing good practical performance tested via simulations. Through controlled simulations, we show that the developed algorithm follows a natural hypothesis that improvement in network connection leads to improvement in performance. An important conclusion is that a simple voting strategy is efficient to find common information.

Appendix A
Proof of Lemma 1

This lemma is also used in slightly varying forms in other papers, for example in [39], [15].

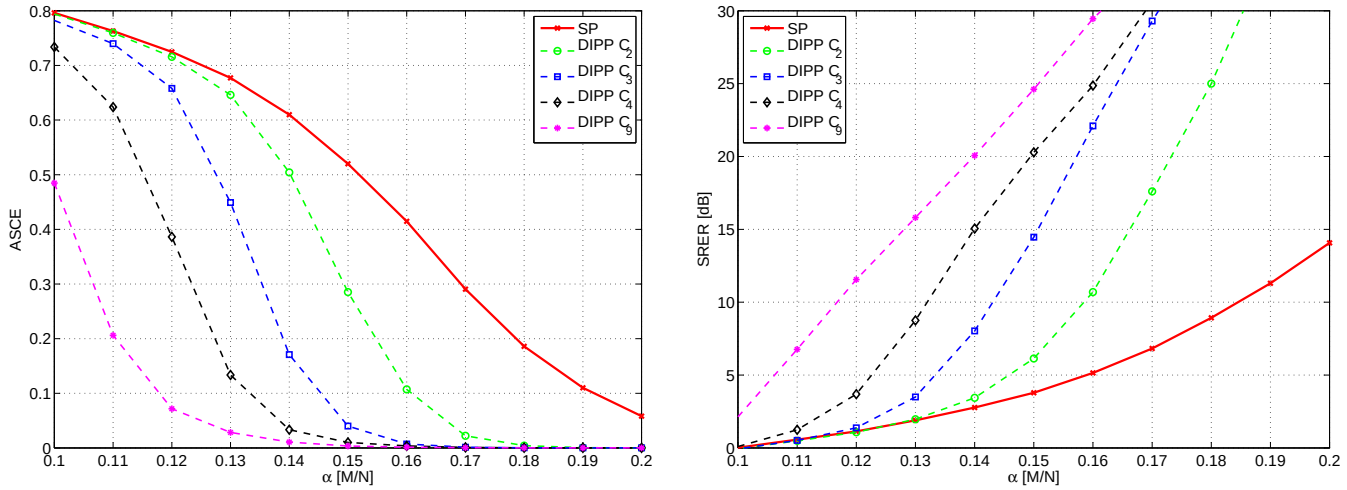

(a) ASCE vs fraction of measurements (b) SRER vs fraction of measurements

Fig. 5. Reconstruction of Gaussian sparse signals at clean condition, by varying network connectivity and fraction of measurements α.

We begin by proving (6)

$$\begin{aligned}
\|\mathbf{x}-\hat{\mathbf{x}}\| &\leq \|\mathbf{x}_{\hat{\mathcal{T}}} - \mathbf{A}_{\hat{\mathcal{T}}}^{\dagger}\mathbf{y}\| + \|\mathbf{x}_{\hat{\mathcal{T}}^c}\| \\
&= \|\mathbf{x}_{\hat{\mathcal{T}}} - \mathbf{A}_{\hat{\mathcal{T}}}^{\dagger}(\mathbf{A}_{\mathcal{T}}\mathbf{x}_{\mathcal{T}} + \mathbf{e})\| + \|\mathbf{x}_{\hat{\mathcal{T}}^c}\| \\
&\leq \|\mathbf{x}_{\hat{\mathcal{T}}} - \mathbf{A}_{\hat{\mathcal{T}}}^{\dagger}\mathbf{A}_{\mathcal{T}}\mathbf{x}_{\mathcal{T}}\| + \|\mathbf{A}_{\hat{\mathcal{T}}}^{\dagger}\mathbf{e}\| + \|\mathbf{x}_{\hat{\mathcal{T}}^c}\| \\
&\overset{(a)}{=} \|\underbrace{\mathbf{x}_{\hat{\mathcal{T}}} - \mathbf{A}_{\hat{\mathcal{T}}}^{\dagger}\mathbf{A}_{\mathcal{T}\cap\hat{\mathcal{T}}}\mathbf{x}_{\mathcal{T}\cap\hat{\mathcal{T}}}}_{=0} - \mathbf{A}_{\hat{\mathcal{T}}}^{\dagger}\mathbf{A}_{\hat{\mathcal{T}}^c}\mathbf{x}_{\hat{\mathcal{T}}^c}\| \\
&\quad + \|\mathbf{A}_{\hat{\mathcal{T}}}^{\dagger}\mathbf{e}\| + \|\mathbf{x}_{\hat{\mathcal{T}}^c}\| \\
&= \|\mathbf{A}_{\hat{\mathcal{T}}}^{\dagger}\mathbf{A}_{\hat{\mathcal{T}}^c}\mathbf{x}_{\hat{\mathcal{T}}^c}\| + \|\mathbf{A}_{\hat{\mathcal{T}}}^{\dagger}\mathbf{e}\| + \|\mathbf{x}_{\hat{\mathcal{T}}^c}\| \\
&\overset{(b)}{\leq} \left(1 + \frac{\delta_{2T}}{1-\delta_T}\right)\|\mathbf{x}_{\hat{\mathcal{T}}^c}\| + \frac{1}{\sqrt{1-\delta_T}}\|\mathbf{e}\| \\
&\overset{(c)}{\leq} \frac{1}{1-\delta_{3T}}\|\mathbf{x}_{\hat{\mathcal{T}}^c}\| + \frac{1}{\sqrt{1-\delta_{3T}}}\|\mathbf{e}\|.
\end{aligned}$$

In the above, we have in (a) used that $\mathbf{A}_{\mathcal{T}}\mathbf{x}_{\mathcal{T}} = \mathbf{A}_{\mathcal{T}\cap\hat{\mathcal{T}}}\mathbf{x}_{\mathcal{T}\cap\hat{\mathcal{T}}} + \mathbf{A}_{\hat{\mathcal{T}}^c}\mathbf{x}_{\hat{\mathcal{T}}^c}$. In (b) we have used proposition 1 and 2, and corollary 1. Lastly, in (c) we have used $\delta_s \leq \delta_{2T} \leq \delta_{3T}$. Now, proving (7) is straight forward

$$\|\mathbf{x}-\hat{\mathbf{x}}\|^2 = \|\mathbf{x}_{\hat{\mathcal{T}}} - \mathbf{A}_{\hat{\mathcal{T}}}^{\dagger}\mathbf{y}\|^2 + \|\mathbf{x}_{\hat{\mathcal{T}}^c}\|^2 \geq \|\mathbf{x}_{\hat{\mathcal{T}}^c}\|^2$$

Taking square-root on both sides gives

$$\|\mathbf{x}-\hat{\mathbf{x}}\| \geq \|\mathbf{x}_{\hat{\mathcal{T}}^c}\|.$$

■

APPENDIX B
PROOF OF LEMMA 2

We will prove

$$\|\mathbf{x}_{\hat{\mathcal{T}}_l^c}\| \leq \frac{1+\delta_{3T}}{1-\delta_{3T}}\|\mathbf{x}_{\check{\mathcal{U}}_l^c}\| + \frac{2}{\sqrt{1-\delta_{3T}}}\|\mathbf{e}\|.$$

Our proof is similar to the proof of Theorem 1 in [39], appendix I in [15] and also appendix C in [40]. Here, we would like to point out that by following ideas from [40], a slightly tighter bound can be formed. However, we abandon those ideas in favor of clarity in the derivations. In this proof we drop the sub-index 'l' for less notational clutter. We start with defining

$$\mathcal{T}_{\Delta} = \check{\mathcal{U}} \setminus \hat{\mathcal{T}}.$$

Observe that $\hat{\mathcal{T}} \subset \check{\mathcal{U}}$. Then, by using $\hat{\mathcal{T}}^c = \check{\mathcal{U}}^c \cup \mathcal{T}_{\Delta}$ we get

$$\|\mathbf{x}_{\hat{\mathcal{T}}^c}\| \leq \|\mathbf{x}_{\check{\mathcal{U}}^c}\| + \|\mathbf{x}_{\mathcal{T}_{\Delta}}\|. \tag{27}$$

Let us consider the following relation,

$$\begin{aligned}
\|\check{\mathbf{x}}_{\mathcal{T}_{\Delta}}\| &= \|\mathbf{x}_{\mathcal{T}_{\Delta}} + (\check{\mathbf{x}}_{\check{\mathcal{U}}} - \mathbf{x}_{\check{\mathcal{U}}})_{\mathcal{T}_{\Delta}}\| \\
&\geq \|\mathbf{x}_{\mathcal{T}_{\Delta}}\| - \|(\check{\mathbf{x}}_{\check{\mathcal{U}}} - \mathbf{x}_{\check{\mathcal{U}}})_{\mathcal{T}_{\Delta}}\|,
\end{aligned}$$

which by rearranging the terms

$$\begin{aligned}
\|\mathbf{x}_{\mathcal{T}_{\Delta}}\| &\leq \|\check{\mathbf{x}}_{\mathcal{T}_{\Delta}}\| + \|(\check{\mathbf{x}}_{\check{\mathcal{U}}} - \mathbf{x}_{\check{\mathcal{U}}})_{\mathcal{T}_{\Delta}}\| \\
&\leq \|\check{\mathbf{x}}_{\mathcal{T}_{\Delta}}\| + \|\check{\mathbf{x}}_{\check{\mathcal{U}}} - \mathbf{x}_{\check{\mathcal{U}}}\|.
\end{aligned} \tag{28}$$

Furthermore, we have that

$$\begin{aligned}
\|\check{\mathbf{x}}_{\mathcal{T}_{\Delta}}\|^2 &= \|\check{\mathbf{x}}_{\mathcal{T}_{\Delta}}\|^2 + \|\check{\mathbf{x}}_{\hat{\mathcal{T}}}\|^2 - \|\check{\mathbf{x}}_{\hat{\mathcal{T}}}\|^2 \\
&= \|\check{\mathbf{x}}\|^2 - \|\check{\mathbf{x}}_{\hat{\mathcal{T}}}\|^2 \\
&= \|\check{\mathbf{x}}_{\check{\mathcal{U}}\setminus\mathcal{T}}\|^2 + \|\check{\mathbf{x}}_{\mathcal{T}}\|^2 - \|\check{\mathbf{x}}_{\hat{\mathcal{T}}}\|^2 \\
&\overset{(a)}{\leq} \|\check{\mathbf{x}}_{\check{\mathcal{U}}\setminus\mathcal{T}}\|^2,
\end{aligned}$$

where we in (a) have used that $\|\check{\mathbf{x}}_{\mathcal{T}}\|^2 - \|\check{\mathbf{x}}_{\hat{\mathcal{T}}}\|^2 \leq 0$, by definition. Taking square-root on both sides gives

$$\begin{aligned}
\|\check{\mathbf{x}}_{\mathcal{T}_{\Delta}}\| &\leq \|\check{\mathbf{x}}_{\check{\mathcal{U}}\setminus\mathcal{T}}\| \\
&= \|\check{\mathbf{x}}_{\check{\mathcal{U}}\setminus\mathcal{T}} - \mathbf{x}_{\check{\mathcal{U}}\setminus\mathcal{T}}\| \\
&= \|(\check{\mathbf{x}}_{\check{\mathcal{U}}} - \mathbf{x}_{\check{\mathcal{U}}})_{\check{\mathcal{U}}\setminus\mathcal{T}}\| \\
&\leq \|\check{\mathbf{x}}_{\check{\mathcal{U}}} - \mathbf{x}_{\check{\mathcal{U}}}\|.
\end{aligned} \tag{29}$$

Combining (29) with (28) gives

$$\|\mathbf{x}_{\mathcal{T}_{\Delta}}\| \leq 2\|\check{\mathbf{x}}_{\check{\mathcal{U}}} - \mathbf{x}_{\check{\mathcal{U}}}\|. \tag{30}$$

Studying RHS of (30)

$$\begin{aligned}\|\mathbf{x}_{\check{\mathcal{U}}}-\check{\mathbf{x}}_{\check{\mathcal{U}}}\| &= \|\mathbf{x}_{\check{\mathcal{U}}}-\mathbf{A}_{\check{\mathcal{U}}}^{\dagger}(\mathbf{A}\mathbf{x}+\mathbf{e})\| \\ &= \|\mathbf{x}_{\check{\mathcal{U}}}-\mathbf{A}_{\check{\mathcal{U}}}^{\dagger}(\mathbf{A}_{\check{\mathcal{U}}}\mathbf{x}_{\check{\mathcal{U}}}+\mathbf{A}_{\check{\mathcal{U}}^c}\mathbf{x}_{\check{\mathcal{U}}^c}+\mathbf{e})\| \\ &= \|\mathbf{A}_{\check{\mathcal{U}}}^{\dagger}\mathbf{A}_{\check{\mathcal{U}}^c}\mathbf{x}_{\check{\mathcal{U}}^c}+\mathbf{A}_{\check{\mathcal{U}}}^{\dagger}\mathbf{e}\| \\ &\leq \|\mathbf{A}_{\check{\mathcal{U}}}^{\dagger}\mathbf{A}_{\check{\mathcal{U}}^c}\mathbf{x}_{\check{\mathcal{U}}^c}\|+\|\mathbf{A}_{\check{\mathcal{U}}}^{\dagger}\mathbf{e}\| \\ &= \|(\mathbf{A}_{\check{\mathcal{U}}}^{*}\mathbf{A}_{\check{\mathcal{U}}})^{-1}\mathbf{A}_{\check{\mathcal{U}}}^{*}\mathbf{A}_{\check{\mathcal{U}}^c}\mathbf{x}_{\check{\mathcal{U}}^c}\|+\|\mathbf{A}_{\check{\mathcal{U}}}^{\dagger}\mathbf{e}\| \\ &\overset{(a)}{\leq} \frac{\delta_{3T}}{1-\delta_{2T}}\|\mathbf{x}_{\check{\mathcal{U}}^c}\|+\frac{1}{\sqrt{1-\delta_{2T}}}\|\mathbf{e}\|, \end{aligned} \tag{31}$$

where we in (a) have used (3d) and (3b) of proposition 1, and corollary 1. Now, by combining (31), (30) and (27) we get

$$\begin{aligned}\|\mathbf{x}_{\hat{\mathcal{T}}^c}\| &\leq \left(1+\frac{2\delta_{3T}}{1-\delta_{2T}}\right)\|\mathbf{x}_{\check{\mathcal{U}}^c}\|+\frac{2}{\sqrt{1-\delta_{2T}}}\|\mathbf{e}\| \\ &\overset{(a)}{\leq} \frac{1+\delta_{3T}}{1-\delta_{3T}}\|\mathbf{x}_{\check{\mathcal{U}}^c}\|+\frac{2}{\sqrt{1-\delta_{3T}}}\|\mathbf{e}\|,\end{aligned}$$

where we in (a) have used that $\delta_{2T}\leq\delta_{3T}$. ■

APPENDIX C
PROOF OF LEMMA 4

We will show that

$$\|\mathbf{x}_{\tilde{\mathcal{U}}_l^c}\| \leq \frac{2\delta_{3T}}{(1-\delta_{3T})^2}\|\mathbf{x}_{\hat{\mathcal{T}}_{l-1}^c}\|+\frac{2\sqrt{1+\delta_{3T}}}{1-\delta_{3T}}\|\mathbf{e}\|.$$

Our proof is similar to the proof in appendix H in [15] and the proof in appendix B in [40]. Here, we would like to point out that by following ideas from [40], a slightly tighter bound can be formed. However, we abandon those ideas in favor of clarity in the derivations. We start with

$$\begin{aligned}\mathbf{r}_{l-1} &= \mathtt{res}(\mathbf{y},\mathbf{A}_{\hat{\mathcal{T}}_{l-1}}) \\ &\overset{(a)}{=} \mathtt{res}(\mathbf{A}_{\hat{\mathcal{T}}_{l-1}^c}\mathbf{x}_{\hat{\mathcal{T}}_{l-1}^c},\mathbf{A}_{\hat{\mathcal{T}}_{l-1}}) \\ &\quad + \mathtt{res}(\mathbf{A}_{\hat{\mathcal{T}}_{l-1}}\mathbf{x}_{\hat{\mathcal{T}}_{l-1}},\mathbf{A}_{\hat{\mathcal{T}}_{l-1}})+\mathtt{res}(\mathbf{e},\mathbf{A}_{\hat{\mathcal{T}}_{l-1}}) \\ &\overset{(b)}{=} \mathtt{res}(\mathbf{A}_{\hat{\mathcal{T}}_{l-1}^c}\mathbf{x}_{\hat{\mathcal{T}}_{l-1}^c},\mathbf{A}_{\hat{\mathcal{T}}_{l-1}})+\mathtt{res}(\mathbf{e},\mathbf{A}_{\hat{\mathcal{T}}_{l-1}}).\end{aligned} \tag{32}$$

Here, we have in (a) used that $\Omega = \hat{\mathcal{T}}\cup\hat{\mathcal{T}}^c$ and that the residual operator is linear. In (b) we have used that $\mathtt{res}(\mathbf{A}_{\hat{\mathcal{T}}_{l-1}}\mathbf{x}_{\hat{\mathcal{T}}_{l-1}},\mathbf{A}_{\hat{\mathcal{T}}_{l-1}}) = \mathbf{A}_{\hat{\mathcal{T}}_{l-1}}\mathbf{x}_{\hat{\mathcal{T}}_{l-1}} - \mathbf{A}_{\hat{\mathcal{T}}_{l-1}}\mathbf{A}_{\hat{\mathcal{T}}_{l-1}}^{\dagger}\mathbf{A}_{\hat{\mathcal{T}}_{l-1}}\mathbf{x}_{\hat{\mathcal{T}}_{l-1}} = 0$. We now study the first term of RHS in (32)

$$\begin{aligned}&\mathtt{res}(\mathbf{A}_{\hat{\mathcal{T}}_{l-1}^c}\mathbf{x}_{\hat{\mathcal{T}}_{l-1}^c},\mathbf{A}_{\hat{\mathcal{T}}_{l-1}}) \\ &\quad= \mathbf{A}_{\hat{\mathcal{T}}_{l-1}^c}\mathbf{x}_{\hat{\mathcal{T}}_{l-1}^c}-\mathbf{A}_{\hat{\mathcal{T}}_{l-1}}\mathbf{A}_{\hat{\mathcal{T}}_{l-1}}^{\dagger}\mathbf{A}_{\hat{\mathcal{T}}_{l-1}^c}\mathbf{x}_{\hat{\mathcal{T}}_{l-1}^c} \\ &\quad= \begin{bmatrix}\mathbf{A}_{\hat{\mathcal{T}}_{l-1}^c} & \mathbf{A}_{\hat{\mathcal{T}}_{l-1}}\end{bmatrix}\begin{bmatrix}\mathbf{x}_{\hat{\mathcal{T}}_{l-1}^c} \\ -\mathbf{A}_{\hat{\mathcal{T}}_{l-1}}^{\dagger}\mathbf{A}_{\hat{\mathcal{T}}_{l-1}^c}\mathbf{x}_{\hat{\mathcal{T}}_{l-1}^c}\end{bmatrix} \\ &\quad= \mathbf{A}\mathbf{q}_{l-1}.\end{aligned} \tag{33}$$

Observe that $\mathbf{q}_{l-1}$ is at most $2T$-sparse with support-set $\mathcal{T}\cup\hat{\mathcal{T}}_{l-1}$. Thus, we can write that

$$\mathbf{r}_{l-1} = \mathbf{A}\mathbf{q}_{l-1}+\mathtt{res}(\mathbf{e},\mathbf{A}_{\hat{\mathcal{T}}_{l-1}}). \tag{34}$$

Now, by the definition of $\grave{\mathcal{T}}_l$, we have that

$$\begin{aligned}\|\mathbf{A}_{\grave{\mathcal{T}}_l}^{*}\mathbf{r}_{l-1}\| &\geq \|\mathbf{A}_{\mathcal{T}}^{*}\mathbf{r}_{l-1}\| \geq \|\mathbf{A}_{\mathcal{T}\setminus\hat{\mathcal{T}}_{l-1}}^{*}\mathbf{r}_{l-1}\| \\ &\overset{(a)}{\geq} \|\mathbf{A}_{\mathcal{T}\setminus\hat{\mathcal{T}}_{l-1}}^{*}\mathbf{A}\mathbf{q}_{l-1}\|-\|\mathbf{A}_{\mathcal{T}\setminus\hat{\mathcal{T}}_{l-1}}^{*}\mathtt{res}(\mathbf{e},\mathbf{A}_{\hat{\mathcal{T}}_{l-1}})\| \\ &\overset{(b)}{\geq} \|\mathbf{A}_{\mathcal{T}\setminus\hat{\mathcal{T}}_{l-1}}^{*}\mathbf{A}\mathbf{q}_{l-1}\|-\sqrt{1+\delta_T}\|\mathbf{e}\|.\end{aligned} \tag{35}$$

We have in (a) used (34) and the reversed triangle inequality, while we in (b) have used (3a) in proposition 1 and that $\|\mathtt{res}(\mathbf{e},\mathbf{A}_{\hat{\mathcal{T}}_{l-1}})\|\leq\|\mathbf{e}\|$. Similarly we can provide the following upper-bound

$$\begin{aligned}\|\mathbf{A}_{\grave{\mathcal{T}}_l}^{*}\mathbf{r}_{l-1}\| &\overset{(a)}{\leq} \|\mathbf{A}_{\grave{\mathcal{T}}_l}^{*}\mathbf{A}\mathbf{q}_{l-1}\|+\|\mathbf{A}_{\grave{\mathcal{T}}_l}^{*}\mathtt{res}(\mathbf{e},\mathbf{A}_{\hat{\mathcal{T}}_{l-1}})\| \\ &\overset{(b)}{\leq} \|\mathbf{A}_{\grave{\mathcal{T}}_l}^{*}\mathbf{A}\mathbf{q}_{l-1}\|+\sqrt{1+\delta_T}\|\mathbf{e}\|.\end{aligned} \tag{36}$$

We have in (a) used (34) and the triangle inequality, while we in (b) have used (3a) in proposition 1 and that $\|\mathtt{res}(\mathbf{e},\mathbf{A}_{\hat{\mathcal{T}}_{l-1}})\|\leq\|\mathbf{e}\|$.

Combining (35) and (36) gives

$$\|\mathbf{A}_{\grave{\mathcal{T}}_l}^{*}\mathbf{A}\mathbf{q}_{l-1}\|+2\sqrt{1+\delta_T}\|\mathbf{e}\| \geq \|\mathbf{A}_{\mathcal{T}\setminus\hat{\mathcal{T}}_{l-1}}^{*}\mathbf{A}\mathbf{q}_{l-1}\|.$$

We remove the common columns in $\mathbf{A}_{\grave{\mathcal{T}}_l}$ and $\mathbf{A}_{\mathcal{T}\setminus\hat{\mathcal{T}}_{l-1}}$ on both sides (observe that $\hat{\mathcal{T}}_{l-1}\not\subseteq\grave{\mathcal{T}}_l$)

$$\begin{aligned}\|\mathbf{A}_{\grave{\mathcal{T}}_l\setminus\mathcal{T}}^{*}\mathbf{A}\mathbf{q}_{l-1}\|+2\sqrt{1+\delta_T}\|\mathbf{e}\| &\geq \|\mathbf{A}_{(\mathcal{T}\setminus\hat{\mathcal{T}}_{l-1})\setminus\grave{\mathcal{T}}_l}^{*}\mathbf{A}\mathbf{q}_{l-1}\| \\ &\overset{(a)}{=} \|\mathbf{A}_{\mathcal{T}\setminus\tilde{\mathcal{U}}_l}^{*}\mathbf{A}\mathbf{q}_{l-1}\|,\end{aligned} \tag{37}$$

where (a) follows from that $(\mathcal{T}\setminus\hat{\mathcal{T}}_{l-1})\setminus\grave{\mathcal{T}}_l = \mathcal{T}\setminus(\hat{\mathcal{T}}_{l-1}\cup\grave{\mathcal{T}}_l) = \mathcal{T}\setminus\tilde{\mathcal{U}}_l$. We now upper-bound the first term of the LHS of (37).

$$\begin{aligned}\|\mathbf{A}_{\grave{\mathcal{T}}_l\setminus\mathcal{T}}^{*}\mathbf{A}\mathbf{q}_{l-1}\| &\overset{(a)}{=} \|\mathbf{A}_{\grave{\mathcal{T}}_l\setminus\mathcal{T}}^{*}\mathbf{A}_{\mathcal{T}\cup\hat{\mathcal{T}}_{l-1}}(\mathbf{q}_{l-1})_{\mathcal{T}\cup\hat{\mathcal{T}}_{l-1}}\| \\ &\leq \|\mathbf{A}_{\grave{\mathcal{T}}_l\setminus\mathcal{T}}^{*}\mathbf{A}_{\mathcal{T}\cup\hat{\mathcal{T}}_{l-1}}\|\|(\mathbf{q}_{l-1})_{\mathcal{T}\cup\hat{\mathcal{T}}_{l-1}}\| \\ &\overset{(b)}{\leq} \delta_{3T}\|\mathbf{q}_{l-1}\|.\end{aligned} \tag{38}$$

In (a), we used that $\mathbf{q}_{l-1}$ has support only over $\mathcal{T}\cup\hat{\mathcal{T}}_{l-1}$ from (33), and in (b) we used proposition 2. Furthermore, we lower-bound the RHS of (37)

$$\begin{aligned}&\|\mathbf{A}_{\mathcal{T}\setminus\tilde{\mathcal{U}}_l}^{*}\mathbf{A}\mathbf{q}_{l-1}\| \\ &\overset{(a)}{=} \|\mathbf{A}_{\mathcal{T}\setminus\tilde{\mathcal{U}}_l}^{*}\mathbf{A}_{\mathcal{T}\cup\hat{\mathcal{T}}_{l-1}}(\mathbf{q}_{l-1})_{\mathcal{T}\cup\hat{\mathcal{T}}_{l-1}}\| \\ &= \|\mathbf{A}_{\mathcal{T}\setminus\tilde{\mathcal{U}}_l}^{*}\mathbf{A}_{(\mathcal{T}\cup\hat{\mathcal{T}}_{l-1})\setminus\tilde{\mathcal{U}}_l}(\mathbf{q}_{l-1})_{(\mathcal{T}\cup\hat{\mathcal{T}}_{l-1})\setminus\tilde{\mathcal{U}}_l} \\ &\quad+\mathbf{A}_{\mathcal{T}\setminus\tilde{\mathcal{U}}_l}^{*}\mathbf{A}_{(\mathcal{T}\cup\hat{\mathcal{T}}_{l-1})\cap\tilde{\mathcal{U}}_l}(\mathbf{q}_{l-1})_{(\mathcal{T}\cup\hat{\mathcal{T}}_{l-1})\cap\tilde{\mathcal{U}}_l}\| \\ &\overset{(b)}{\geq} \|\mathbf{A}_{\mathcal{T}\setminus\tilde{\mathcal{U}}_l}^{*}\mathbf{A}_{\mathcal{T}\setminus\tilde{\mathcal{U}}_l}(\mathbf{q}_{l-1})_{\mathcal{T}\setminus\tilde{\mathcal{U}}_l}\| \\ &\quad-\|\mathbf{A}_{\mathcal{T}\setminus\tilde{\mathcal{U}}_l}^{*}\mathbf{A}_{(\mathcal{T}\cup\hat{\mathcal{T}}_{l-1})\cap\tilde{\mathcal{U}}_l}(\mathbf{q}_{l-1})_{(\mathcal{T}\cup\hat{\mathcal{T}}_{l-1})\cap\tilde{\mathcal{U}}_l}\| \\ &\overset{(c)}{\geq} (1-\delta_T)\|(\mathbf{q}_{l-1})_{\mathcal{T}\setminus\tilde{\mathcal{U}}_l}\| \\ &\quad-\|\mathbf{A}_{\mathcal{T}\setminus\tilde{\mathcal{U}}_l}^{*}\mathbf{A}_{(\mathcal{T}\cup\hat{\mathcal{T}}_{l-1})\cap\tilde{\mathcal{U}}_l}\|\|(\mathbf{q}_{l-1})_{(\mathcal{T}\cup\hat{\mathcal{T}}_{l-1})\cap\tilde{\mathcal{U}}_l}\| \\ &\overset{(d)}{\geq} (1-\delta_{3T})\|(\mathbf{q}_{l-1})_{\mathcal{T}\setminus\tilde{\mathcal{U}}_l}\|-\delta_{3T}\|(\mathbf{q}_{l-1})_{(\mathcal{T}\cup\hat{\mathcal{T}}_{l-1})\cap\tilde{\mathcal{U}}_l}\| \\ &\geq (1-\delta_{3T})\|(\mathbf{q}_{l-1})_{\mathcal{T}\setminus\tilde{\mathcal{U}}_l}\|-\delta_{3T}\|\mathbf{q}_{l-1}\|.\end{aligned} \tag{39}$$

In (a), we used that $\mathbf{q}_{l-1}$ has support over $\mathcal{T}\cup\hat{\mathcal{T}}_{l-1}$. In (b), we used the reversed triangle inequality. In (c), for the

first term (3c) of proposition 1 is used and the second term follows from that the spectral norm is sub-multiplicative. In (d) proposition 2 is applied (note that $\mathcal{T}\backslash\tilde{\mathcal{U}}_l$ does not intersect with $(\mathcal{T}\cup\hat{\mathcal{T}}_{l-1})\cap\tilde{\mathcal{U}}_l$) together with $\delta_T\leq\delta_{2T}\leq\delta_{3T}$.

Now, by substituting (38) and (39) into (37), we get

$$2\delta_{3T}\|\mathbf{q}_{l-1}\|+2\sqrt{1+\delta_{3T}}\|\mathbf{e}\|\geq(1-\delta_{3T})\|(\mathbf{q}_{l-1})_{\mathcal{T}\backslash\tilde{\mathcal{U}}_l}\|, \tag{40}$$

where we also applied that $\delta_T\leq\delta_{3T}$. We now observe that

$$\begin{aligned}\|\mathbf{q}_{l-1}\|&=\left\|\begin{bmatrix}\mathbf{x}_{\hat{\mathcal{T}}^{\mathsf{c}}_{l-1}}\\ -\mathbf{A}^{\dagger}_{\hat{\mathcal{T}}_{l-1}}\mathbf{A}_{\hat{\mathcal{T}}^{\mathsf{c}}_{l-1}}\mathbf{x}_{\hat{\mathcal{T}}^{\mathsf{c}}_{l-1}}\end{bmatrix}\right\|\\&\leq\|\mathbf{x}_{\hat{\mathcal{T}}^{\mathsf{c}}_{l-1}}\|+\|\mathbf{A}^{\dagger}_{\hat{\mathcal{T}}_{l-1}}\mathbf{A}_{\hat{\mathcal{T}}^{\mathsf{c}}_{l-1}}\mathbf{x}_{\hat{\mathcal{T}}^{\mathsf{c}}_{l-1}}\|\\&=\|\mathbf{x}_{\hat{\mathcal{T}}^{\mathsf{c}}_{l-1}}\|+\|(\mathbf{A}^{*}_{\hat{\mathcal{T}}_{l-1}}\mathbf{A}_{\hat{\mathcal{T}}_{l-1}})^{-1}\mathbf{A}^{*}_{\hat{\mathcal{T}}_{l-1}}\mathbf{A}_{\hat{\mathcal{T}}^{\mathsf{c}}_{l-1}}\mathbf{x}_{\hat{\mathcal{T}}^{\mathsf{c}}_{l-1}}\|\\&\overset{(a)}{\leq}\|\mathbf{x}_{\hat{\mathcal{T}}^{\mathsf{c}}_{l-1}}\|+\frac{\delta_{2T}}{1-\delta_T}\|\mathbf{x}_{\hat{\mathcal{T}}^{\mathsf{c}}_{l-1}}\|\\&\overset{(b)}{\leq}\left(1+\frac{\delta_{3T}}{1-\delta_{3T}}\right)\|\mathbf{x}_{\hat{\mathcal{T}}^{\mathsf{c}}_{l-1}}\|=\frac{1}{1-\delta_{3T}}\|\mathbf{x}_{\hat{\mathcal{T}}^{\mathsf{c}}_{l-1}}\|.\end{aligned} \tag{41}$$

In (a) we have used (3d) of proposition 1 and corollary 1. In (b) we have used that $\delta_T\leq\delta_{2T}\leq\delta_{3T}$. Furthermore, we have

$$\begin{aligned}\|(\mathbf{q}_{l-1})_{\mathcal{T}\backslash\tilde{\mathcal{U}}_l}\|&=\left\|\begin{bmatrix}\mathbf{x}_{\hat{\mathcal{T}}^{\mathsf{c}}_{l-1}}\\ -\mathbf{A}^{\dagger}_{\hat{\mathcal{T}}_{l-1}}\mathbf{A}_{\hat{\mathcal{T}}^{\mathsf{c}}_{l-1}}\mathbf{x}_{\hat{\mathcal{T}}^{\mathsf{c}}_{l-1}}\end{bmatrix}_{\mathcal{T}\backslash\tilde{\mathcal{U}}_l}\right\|\\&\overset{(a)}{=}\|(\mathbf{x}_{\hat{\mathcal{T}}^{\mathsf{c}}_{l-1}})_{\mathcal{T}\backslash\tilde{\mathcal{U}}_l}\|\\&=\|\mathbf{x}_{\tilde{\mathcal{U}}^{\mathsf{c}}_l}\|,\end{aligned} \tag{42}$$

where we in (a) have used that $\mathcal{T}\setminus\tilde{\mathcal{U}}_l\subseteq\mathcal{T}\setminus\hat{\mathcal{T}}_{l-1}\subset\hat{\mathcal{T}}^{\mathsf{c}}_{l-1}$. By substituting (41) and (42) into (40), we get

$$\frac{2\delta_{3T}}{1-\delta_{3T}}\|\mathbf{x}_{\hat{\mathcal{T}}^{\mathsf{c}}_{l-1}}\|+2\sqrt{1+\delta_{3T}}\|\mathbf{e}\|\geq(1-\delta_{3T})\|\mathbf{x}_{\tilde{\mathcal{U}}^{\mathsf{c}}_l}\|,$$

which equivalently can be written as

$$\|\mathbf{x}_{\tilde{\mathcal{U}}^{\mathsf{c}}_l}\|\leq\frac{2\delta_{3T}}{(1-\delta_{3T})^2}\|\mathbf{x}_{\hat{\mathcal{T}}^{\mathsf{c}}_{l-1}}\|+\frac{2\sqrt{1+\delta_{3T}}}{1-\delta_{3T}}\|\mathbf{e}\|.$$

■

APPENDIX D
PROOFS FOR DPP

Proof of Proposition 6: To find the recurrence inequality for DIPP, we use the performance bound for SIPP and the `expansion` jointly, presented in proposition 4 and proposition 5. These two propositions have no outer loop iteration parameter k. Thus, we introduce proposition 4 with the outer loop iteration counter:

$$\|(\mathbf{x}_{\mathsf{p}})_{\hat{\mathcal{T}}^{\mathsf{c}}_{\mathsf{p},k}}\|\leq\frac{b_{\text{SIPP}}}{1-a_{\text{SIPP}}}\|(\mathbf{x}_{\mathsf{p}})_{\mathcal{T}^{\mathsf{c}}_{\mathsf{p},\text{si},k}}\|+\frac{1-a_{\text{SIPP}}+c_{\text{SIPP}}}{1-a_{\text{SIPP}}}\|\mathbf{e}_{\mathsf{p}}\|. \tag{43}$$

Observe that this relation requires that $a_{\text{SIPP}}<1$. We also introduce proposition 5 with iteration counter:

$$\|(\mathbf{x}_{\mathsf{p}})_{\mathcal{T}^{\mathsf{c}}_{\mathsf{p},\text{si},k}}\|\leq a_{\mathsf{co}}\|(\mathbf{x}_{\mathsf{p}})_{\hat{\mathcal{T}}^{\mathsf{c}}_{\mathsf{p},k-1}}\|. \tag{44}$$

By combining (43) and (44), we get

$$\|(\mathbf{x}_{\mathsf{p}})_{\hat{\mathcal{T}}^{\mathsf{c}}_{\mathsf{p},k}}\|<a_{\mathsf{co}}\frac{b_{\text{SIPP}}}{1-a_{\text{SIPP}}}\|(\mathbf{x}_{\mathsf{p}})_{\hat{\mathcal{T}}^{\mathsf{c}}_{\mathsf{p},k-1}}\|+\frac{1-a_{\text{SIPP}}+c_{\text{SIPP}}}{1-a_{\text{SIPP}}}\|\mathbf{e}_{\mathsf{p}}\|,$$

where we have assumed that $a_{\text{SIPP}}<1$. ■

Proof of Proposition 7: We start with proving (25), by iteratively applying Proposition 6

$$\begin{aligned}&\|(\mathbf{x}_{\mathsf{p}})_{\hat{\mathcal{T}}^{\mathsf{c}}_{\mathsf{p},k}}\|\\&\leq\frac{a_{\mathsf{co}}b_{\text{SIPP}}}{1-a_{\text{SIPP}}}\|(\mathbf{x}_{\mathsf{p}})_{\hat{\mathcal{T}}^{\mathsf{c}}_{\mathsf{p},k-1}}\|+\frac{1-a_{\text{SIPP}}+c_{\text{SIPP}}}{1-a_{\text{SIPP}}}\|\mathbf{e}_{\mathsf{p}}\|\\&\leq\frac{a_{\mathsf{co}}b_{\text{SIPP}}}{1-a_{\text{SIPP}}}\left(\frac{a_{\mathsf{co}}b_{\text{SIPP}}}{1-a_{\text{SIPP}}}\|(\mathbf{x}_{\mathsf{p}})_{\hat{\mathcal{T}}^{\mathsf{c}}_{\mathsf{p},k-2}}\|\right.\\&\quad\left.+\frac{1-a_{\text{SIPP}}+c_{\text{SIPP}}}{1-a_{\text{SIPP}}}\|\mathbf{e}_{\mathsf{p}}\|\right)+\frac{1-a_{\text{SIPP}}+c_{\text{SIPP}}}{1-a_{\text{SIPP}}}\|\mathbf{e}\|\\&\overset{(a)}{\leq}\left(\frac{a_{\mathsf{co}}b_{\text{SIPP}}}{1-a_{\text{SIPP}}}\right)^{k^*}\|(\mathbf{x}_{\mathsf{p}})_{\mathcal{T}_{\mathsf{p},k-k^*}}\|\\&\quad+\frac{1-a_{\text{SIPP}}+c_{\text{SIPP}}}{1-a_{\text{SIPP}}}\sum_{i=0}^{k^*-1}\left(\frac{a_{\mathsf{co}}b_{\text{SIPP}}}{1-a_{\text{SIPP}}}\right)^{i}\|\mathbf{e}_{\mathsf{p}}\|.\end{aligned} \tag{45}$$

In (a), we recursively applied the recurrence inequality. We now require that $\frac{a_{\mathsf{co}}b_{\text{SIPP}}}{1-a_{\text{SIPP}}}<1$, and then plug in $k^*=\left\lceil\log\left(\frac{\|\mathbf{e}\|}{\|\mathbf{x}\|}\right)/\log\left(a_{\mathsf{co}}\frac{b_{\text{SIPP}}}{1-a_{\text{SIPP}}}\right)\right\rceil$ into (45) and use geometric series to get that

$$\begin{aligned}\|(\mathbf{x}_{\mathsf{p}})_{\hat{\mathcal{T}}^{\mathsf{c}}_{\mathsf{p},\text{DIPP}}}\|&\leq\|\mathbf{e}_{\mathsf{p}}\|+\frac{1-a_{\text{SIPP}}+c_{\text{SIPP}}}{1-a_{\text{SIPP}}}\frac{1}{1-\frac{a_{\mathsf{co}}b_{\text{SIPP}}}{1-a_{\text{SIPP}}}}\|\mathbf{e}_{\mathsf{p}}\|\\&=\left(1+\frac{1-a_{\text{SIPP}}+c_{\text{SIPP}}}{(1-a_{\text{SIPP}})(1-a_{\mathsf{co}}b_{\text{SIPP}})}\right)\|\mathbf{e}_{\mathsf{p}}\|\end{aligned}$$

To prove (26), we apply lemma 1

$$\begin{aligned}&\|\mathbf{x}_{\mathsf{p}}-\hat{\mathbf{x}}_{\mathsf{p},\text{DIPP}}\|\\&\leq\frac{1}{1-\delta_{3T}}\|(\mathbf{x}_{\mathsf{p}})_{\hat{\mathcal{T}}^{c}_{\mathsf{p},\text{DIPP}}}\|+\frac{1}{\sqrt{1-\delta_{3T}}}\|\mathbf{e}_{\mathsf{p}}\|\\&=\frac{1}{1-\delta_{3T}}\left(1+\frac{1-a_{\text{SIPP}}+c_{\text{SIPP}}}{(1-a_{\text{SIPP}})(1-a_{\mathsf{co}}b_{\text{SIPP}})}\right)\|\mathbf{e}_{\mathsf{p}}\|\\&\quad+\frac{1}{\sqrt{1-\delta_{3T}}}\|\mathbf{e}_{\mathsf{p}}\|\\&\leq\left(\frac{1-a_{\text{SIPP}}+c_{\text{SIPP}}}{(1-\delta_{3T})(1-a_{\text{SIPP}})(1-a_{\mathsf{co}}b_{\text{SIPP}})}\right.\\&\quad\left.+\frac{2}{1-\delta_{3T}}\right)\|\mathbf{e}_{\mathsf{p}}\|,\end{aligned}$$

which concludes the proof. ■

REFERENCES

[1] D. Sundman, S. Chatterjee, and M. Skoglund, "Parallel pursuit for distributed compressed sensing," in *IEEE Global Conference on Signal and Information Processing (GlobalSIP)*, Austin, Texas, USA, Dec. 2013, pp. –.

[2] D. Donoho, "Compressed sensing," *IEEE Transactions on Information Theory*, vol. 52, pp. 1289–1306, Apr. 2006.

[3] E. J. Candès, J. Romberg, and T. Tao, "Stable signal recovery from incomplete and inaccurate measurements," *Communications on Pure and Applied Mathematics*, vol. 59, pp. 1207–1223, Aug. 2006.

[4] J. Mota, J. Xavier, P. Aguiar, and M. Puschel, "Distributed basis pursuit," *IEEE Transactions on Signal Processing*, vol. 60, pp. 1942–1956, Apr. 2012.

[5] J. Bazerque and G. Giannakis, "Distributed spectrum sensing for cognitive radio networks by exploiting sparsity," *IEEE Transactions on Signal Processing*, vol. 58, pp. 1847–1862, Mar. 2010.
[6] S. Ji, Y. Xue, and L. Carin, "Bayesian compressive sensing," *IEEE Transactions on Signal Processing*, vol. 56, pp. 2346–2356, Jun. 2008.
[7] D. Donoho, A. Maleki, and A. Montanari, "Message-passing algorithms for compressed sensing," *Proceedings of the National Academy of Sciences*, vol. 106, pp. 18 914–18 919, Oct. 2009.
[8] S. Mallat and Z. Zhang, "Matching pursuits with time-frequency dictionaries," *IEEE Transactions on Signal Processing*, vol. 41, pp. 3397–3415, Dec. 1993.
[9] J. Tropp and A. Gilbert, "Signal recovery from random measurements via orthogonal matching pursuit," *IEEE Transactions on Information Theory*, vol. 53, pp. 4655–4666, Dec. 2007.
[10] D. Donoho, Y. Tsaig, I. Drori, and J.-L. Starck, "Sparse solution of underdetermined systems of linear equations by stagewise orthogonal matching pursuit," *IEEE Transactions on Information Theory*, vol. 58, pp. 1094–1121, Feb. 2012.
[11] S. Chatterjee, D. Sundman, M. Vehkaperä, and M.Skoglund, "Projection-based and look-ahead strategies for atom selection," *IEEE Transactions on Signal Processing*, vol. 60, pp. 634–647, Feb. 2012.
[12] D. Sundman, S. Chatterjee, and M. Skoglund, "Frogs: A serial reversible greedy search algorithm," in *IEEE Swedish Communication Technologies Workshop (Swe-CTW)*, Lund, Sweden, Mar. 2012, pp. 40–45.
[13] D. Needell and R. Vershynin, "Signal recovery from incomplete and inaccurate measurements via regularized orthogonal matching pursuit," *IEEE Journal of Selected Topics in Signal Processing*, vol. 4, pp. 310–316, Mar. 2010.
[14] D. Needell and J. A. Tropp, "Cosamp: Iterative signal recovery from incomplete and inaccurate samples," *Applied and Computational Harmonic Analysis*, vol. 26, pp. 301–321, Apr. 2009.
[15] W. Dai and O. Milenkovic, "Subspace pursuit for compressive sensing signal reconstruction," *IEEE Transactions on Information Theory*, vol. 55, pp. 2230–2249, May 2009.
[16] D. Sundman, S. Chatterjee, and M. Skoglund, "Look ahead parallel pursuit," in *IEEE Swedish Communication Technologies Workshop (Swe-CTW)*, Stockholm, Sweden, Oct. 2011, pp. 114–117.
[17] J. Tropp, A. Gilbert, and M. Strauss, "Algorithms for simultaneous sparse approximation. part i: Greedy pursuit," *Signal Processing*, vol. 86, pp. 572–588, Mar. 2006.
[18] A. Rakotomamonjy, "Surveying and comparing simultaneous sparse approximation (or group-lasso) algorithms," *Signal Processing*, vol. 91, pp. 1505–1526, Jul. 2011.
[19] D. Leviatan and V. Temlyakov, "Simultaneous approximation by greedy algorithms," *Advances in Computational Mathematics*, vol. 25, pp. 73–90, Jul. 2006.
[20] S. Cotter, B. Rao, K. Engan, and K. Kreutz-Delgado., "Sparse solutions to linear inverse problems with multiple measurement vectors," *IEEE Transactions on Signal Processing*, vol. 53, pp. 2477–2488, Jul. 2005.
[21] J. Chen and X. Huo, "Theoretical results on sparse representations of multiple-measurement vectors," *IEEE Transactions on Signal Processing*, vol. 54, pp. 4634–4643, Dec. 2006.
[22] D. Sundman, S. Chatterjee, and M. Skoglund, "Greedy pursuits for compressed sensing of jointly sparse signals," in *EURASIP European Signal Processing Conference (EUSIPCO)*, Barcelona, Spain, Aug. 2011, pp. 368–372.
[23] J. Bazerque and G. Giannakis, "Distributed spectrum sensing for cognitive radio networks by exploiting sparsity," *IEEE Transactions on Signal Processing*, vol. 58, pp. 1847–1862, Mar. 2010.
[24] F. Zeng, C. Li, and Z. Tian, "Distributed compressive spectrum sensing in cooperative multihop cognitive networks," vol. 5, pp. 37–48, Feb. 2011.
[25] Q. Ling and T. Zhi, "Decentralized support detection of multiple measurement vectors with joint sparsity," in *IEEE International Conference on Acoustics, Speech and Signal Processing (ICASSP)*, Prague, Czech Republic, May 2011, pp. 2996–2999.
[26] A. Yang, M. Gastpar, R. Bajcsy, and S. Sastry, "Distributed sensor perception via sparse representation," *Proceedings of the IEEE*, vol. 98, pp. 1077–1088, Jun. 2010.
[27] D. Sundman, S. Chatterjee, and M. Skoglund, "On the use of compressive sampling for wide-band spectrum sensing," in *IEEE International Symposium on Signal Processing and Information Technology (ISSPIT)*, Luxor, Egypt, Dec. 2010, pp. 354–359.
[28] D. Sundman, D. Zachariah, and S. Chatterjee, "Distributed predictive subspace pursuit," in *IEEE International Conference on Acoustics, Speech and Signal Processing (ICASSP)*, Vancouver, Canada, May 2013, pp. 4633–4637.
[29] D. Sundman, S. Chatterjee, and M. Skoglund, "A greedy pursuit algorithm for distributed compressed sensing," in *IEEE International Conference on Acoustics, Speech and Signal Processing (ICASSP)*, Kyoto, Japan, Mar. 2012, pp. 2729–2732.
[30] ——, "Distributed greedy pursuit algorithms," *CoRR*, vol. abs/1306.6815, Jul. 2013.
[31] T. Wimalajeewa and P. Varshney, "Cooperative sparsity pattern recovery in distributed networks via distributed-omp," in *IEEE International Conference on Acoustics, Speech and Signal Processing (ICASSP)*, Vancouver, Canada, May 2013, pp. 5288–5292.
[32] W. Zhang, C. Ma, W. Wang, Y. Liu, and L. Zhang, "Side information based orthogonal matching pursuit in distributed compressed sensing," in *IEEE International Conference on Network Infrastructure and Digital Content*, Beijing, China, Jan. 2010, pp. 80–84.
[33] E. Candès and T. Tao, "Decoding by linear programming," *IEEE Transactions on Information Theory*, vol. 51, pp. 4203–4215, Dec. 2005.
[34] A. Kirmani, A. Colaco, F. Wong, and V. Goyal, "CoDAC: A compressive depth acquisition camera framework," in *IEEE International Conference on Acoustics, Speech and Signal Processing (ICASSP)*, Kyoto, Japan, Mar. 2012, pp. 5425–5428.
[35] P. Wu, N. Epain, and C. Jin, "A dereverberation algorithm for spherical microphone arrays using compressed sensing techniques," in *IEEE International Conference on Acoustics, Speech and Signal Processing (ICASSP)*, Kyoto, Japan, Mar. 2012, pp. 4053–4056.
[36] R. Giryes and M. Elad, "Rip-based near-oracle performance guarantees for sp, cosamp, and iht," *IEEE Transactions on Signal Processing*, vol. 60, pp. 1465–1468, Mar. 2012.
[37] G. Reeves and M. Gastpar, "A note on optimal support recovery in compressed sensing," in *Annual Asilomar Conference on Signals, Systems, and Computers*, Pacific Grove, USA, Nov. 2009, pp. 1576–1580.
[38] E. Candès and M. Wakin, "An introduction to compressive sampling," *IEEE Electron Device Letters*, vol. 25, pp. 21–30, Mar. 2008.
[39] S. Ambat, S. Chatterjee, and K. Hari, "Fusion of algorithms for compressed sensing," *IEEE Transactions on Signal Processing*, vol. 61, pp. 3699–3704, Apr. 2013.
[40] R. Giryes and M. Elad, "Rip-based near-oracle performance guarantees for subspace-pursuit, cosamp, and iterative hard-thresholding," *ArXiv e-prints*, vol. abs/1005.4539, May 2010. [Online]. Available: http://arxiv.org/abs/1005.4539